

# Orthonormal polynomial wavelets associated with de la Vallée Poussin-type interpolation on $[-1, 1]$

Woula Themistoclakis<sup>a,\*</sup>, Marc Van Barel<sup>b</sup>

<sup>a</sup>*CNR National Research Council of Italy, IAC Institute for Applied Computing “Mauro Picone”, via P. Castellino, 111, Napoli, 80131, Italy*

<sup>b</sup>*Department of Computer Science, KU Leuven, Celestijnenlaan 200A, Leuven (Heverlee), B-3001, Belgium*

---

## Abstract

Starting from de la Vallée Poussin type (VP) interpolation, the authors have recently introduced a family of interpolating polynomial scaling and wavelet bases generating the approximation and detail spaces of a non-standard multiresolution analysis. Motivated by the fact that, in many applications, orthonormal rather than interpolating bases are preferable, the present study develops a new family of scaling and wavelet polynomials that provide well-localized and orthonormal bases for the same approximation and detail spaces.

We show that the proposed new bases have a behavior very similar to the interpolating bases already introduced, presenting similar features although they are not interpolating but orthonormal. In particular, we study the Fourier projection corresponding to the proposed orthonormal scaling basis, and introduce a discrete version of it by approximating the Fourier-like coefficients. For both continuous and discrete orthogonal projections, we prove the uniform boundedness of the Lebesgue constants and the uniform convergence with an asymptotic rate comparable with the best uniform polynomial approximation.

Numerical experiments confirm the theoretical results and compare the new orthonormal VP scaling and wavelet bases with the interpolating case previously treated by the authors.

*Keywords:* Polynomial wavelets, Orthogonal wavelets on compact intervals, de la Vallée Poussin approximation, Lebesgue constant, Multiresolution methods.

*2020 MSC:* 42C40, 65T60

---

---

\*Corresponding author.

*Email addresses:* [woula.themistoclakis@cnr.it](mailto:woula.themistoclakis@cnr.it) (Woula Themistoclakis), [marc.vanbareel@cs.kuleuven.be](mailto:marc.vanbareel@cs.kuleuven.be) (Marc Van Barel)

## 1. Introduction

In [15] the authors recently introduced a family of interpolating polynomial wavelets  $\psi_{n,k}^m(x)$ ,  $k = 1, \dots, 2n$ , which, at each resolution level  $n \in \mathbb{N}$ , depend on a free parameter  $m = \lfloor \theta n \rfloor$ , with  $\theta \in ]0, 1[$  arbitrarily fixed.

Like other polynomial wavelets (see, e.g., [9, 3, 4]) they are not generated by dilation and translation of a single mother function. Their construction generalizes the trigonometric case considered in [10], and is based on de la Vallée Poussin (VP, for short) interpolation at the Chebyshev nodes:

$$X_n = \left\{ x_k^n = \cos \frac{(2k-1)\pi}{2n}, k = 1, \dots, n \right\}, \quad n \in \mathbb{N}.$$

We recall that VP interpolation, originally introduced in [11], provides near-best polynomials for the uniform approximation of arbitrary continuous functions, reducing the Gibbs phenomenon and yielding optimal error estimates, even with respect to the  $L^1$  norm (see [12, 13, 7, 8] and the references therein for more details).

The basis polynomials of this interpolation process are the fundamental VP polynomials  $\Phi_{n,k}^m$ ,  $k = 1, \dots, n$ , defined in (7). In [15], from the wavelet perspective, they are interpreted as scaling functions at level  $n$  with parameter  $m$ . They satisfy the interpolation property

$$\Phi_{n,k}^m(x_h^n) = \delta_{k,h}, \quad h, k = 1, \dots, n, \quad (1)$$

and form a well-localized, Riesz-stable basis of the sampling space

$$\mathcal{V}_n^m := \text{span}\{\Phi_{n,k}^m \mid k = 1, \dots, n\}. \quad (2)$$

This is a polynomial space of dimension  $n$  which is nested between the canonical spaces  $\mathbb{P}_\nu$  of polynomials of degree at most  $\nu$ , as follows

$$\mathbb{P}_{n-m} \subseteq \mathcal{V}_n^m \subset \mathbb{P}_{n+m-1}, \quad 0 < m < n. \quad (3)$$

As in classical multiresolution analysis, the resolution level  $n$  can be increased or decreased; however, instead of the usual scaling factor 2, multiples of 3 are considered in [15].

More precisely, since  $\mathcal{V}_n^m \subset \mathcal{V}_{3n}^m$ , the detail space  $\mathcal{W}_n^m$  is defined as the orthogonal complement of  $\mathcal{V}_n^m$  in  $\mathcal{V}_{3n}^m$ , i.e.,

$$\mathcal{V}_{3n}^m = \mathcal{V}_n^m \oplus \mathcal{W}_n^m \quad \text{and} \quad \mathcal{V}_n^m \perp \mathcal{W}_n^m, \quad (4)$$

where orthogonality is understood with respect to the following scalar product

$$\langle f, g \rangle_{L_w^2} := \int_{-1}^1 f(x)g(x)w(x)dx, \quad w(x) := \frac{1}{\sqrt{1-x^2}}.$$

Moreover, since  $X_n \subset X_{3n}$ , by considering the set of nodes

$$Y_n := X_{3n} - X_n = \{y_h^n \mid h = 1, \dots, 2n\},$$

a well-localized, Riesz-stable, and interpolatory wavelet basis of the detail space

$$\mathcal{W}_n^m = \text{span}\{\psi_{n,k}^m \mid k = 1, \dots, 2n\} \quad (5)$$

is uniquely determined in [15] by imposing the interpolation property

$$\psi_{n,k}^m(y_h^n) = \delta_{k,h}, \quad h, k = 1, \dots, 2n. \quad (6)$$

Despite the non-orthogonality of the interpolating bases in (2) and (5), efficient decomposition-reconstruction algorithms based on fast discrete cosine transforms were derived in [15] and further generalized in [1]. In the latter, following a non-standard modeling [6], they were applied to image compression and denoising, achieving competitive performance compared to classical wavelets. However, as explained in [1], the non-orthogonality of the interpolating scaling and wavelet bases necessitates the introduction of suitable normalization factors to control the loss of signal energy. In [1], these correction factors were theoretically derived for image compression and experimentally refined for signal denoising. Nevertheless, the problem of determining optimal normalization factors, independent of the specific data and resolution levels, remains open.

In the present paper, we propose a different approach to this problem. For both the approximation and detail spaces at resolution level  $n$ , we define new, well-localized, orthonormal VP scaling and wavelet bases, dependent on the free parameter  $m$ . These bases behave similarly to the previous interpolating VP scaling and wavelet bases but, in addition, are orthonormal, with all the consequent advantages that this property entails.

The paper is organized as follows. Section 2 introduces the orthonormal VP scaling functions. Section 3 studies the Fourier projection and its discrete counterpart based on these scaling functions. Section 4 is devoted to the orthonormal VP wavelet functions. In Section 5, fast decomposition and reconstruction algorithms are developed. Section 6 presents numerical experiments comparing the continuous and discrete Fourier projections with the interpolating VP projection. Section 7 contains the proofs of the theoretical results. Finally, Section 8 presents the conclusions of the present study and outlines directions for future research.

## 2. Orthonormal VP scaling functions

Let us first recall that on the set  $X_n$  of the Chebyshev zeros the interpolating VP scaling functions of level  $n$  and parameter  $m < n$  are defined as follows [15]

$$\Phi_{n,k}^m(x) := \frac{\pi}{n} \sum_{r=0}^{n+m-1} \mu_{n,r}^m p_r(x_k^n) p_r(x), \quad k = 1, \dots, n \quad x \in [-1, 1], \quad (7)$$

where

$$\mu_{n,r}^m := \begin{cases} 1 & \text{if } 0 \leq r \leq n - m \\ \frac{m + n - r}{2m} & \text{if } n - m < r < n + m \\ 0 & \text{otherwise} \end{cases} \quad (8)$$

and  $p_n$  denotes the orthonormal Chebyshev polynomial of the first kind and degree  $n$ , namely

$$p_n(x) := \cos(n \arccos x) \begin{cases} \sqrt{1/\pi} & \text{if } n = 0 \\ \sqrt{2/\pi} & \text{if } n > 0 \end{cases} \quad |x| \leq 1, \quad n = 0, 1, \dots \quad (9)$$

In Figure 1, the polynomials  $\Phi_{13,3}^6$ ,  $\Phi_{13,7}^6$  and  $\Phi_{13,11}^6$  are plotted. Note the interpolation property (1) at the Chebyshev zeros of degree 13 marked with circles.

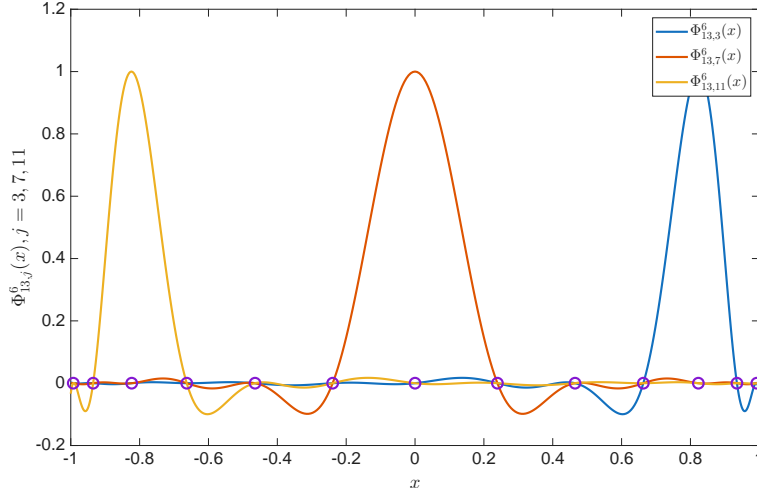


Figure 1: The interpolating VP scaling functions  $\Phi_{n,k}^m$  for  $n = 13$ ,  $m = 6$ , and  $k = 3, 7, 11$ . The open dots denote the set of nodes  $X_n$ .

It is known that the scaling functions in (7) constitute an interpolating Riesz–basis of the approximation space (2), which is also generated by the following rearrangement of the Chebyshev polynomials

$$q_{n,r}^m(x) := \begin{cases} p_r(x) & \text{if } 0 \leq r \leq n - m, \\ \mu_{n,r}^m p_r(x) - \mu_{n,2n-r}^m p_{2n-r}(x) & \text{if } n - m < r < n, \end{cases} \quad (10)$$

These polynomials constitute an orthogonal basis of  $\mathcal{V}_n^m$  satisfying

$$\langle q_{n,r}^m, q_{n,s}^m \rangle_{L_w^2} = \delta_{r,s} \cdot \nu_{n,r}^m, \quad r, s = 0, 1, \dots, n - 1, \quad (11)$$

$$\nu_{n,r}^m := \begin{cases} 1 & \text{if } 0 \leq r \leq n - m, \\ \frac{m^2 + (n - r)^2}{2m^2} & \text{if } n - m < r < n, \end{cases} \quad r = 0, 1, \dots, n - 1. \quad (12)$$

Moreover, we recall the following formula for the change of bases

$$\Phi_{n,k}^m(x) = \frac{\pi}{n} \sum_{r=0}^{n-1} p_r(x_k^n) q_{n,r}^m(x), \quad k = 1, 2, \dots, n, \quad (13)$$

and the inverse formula given in (71).

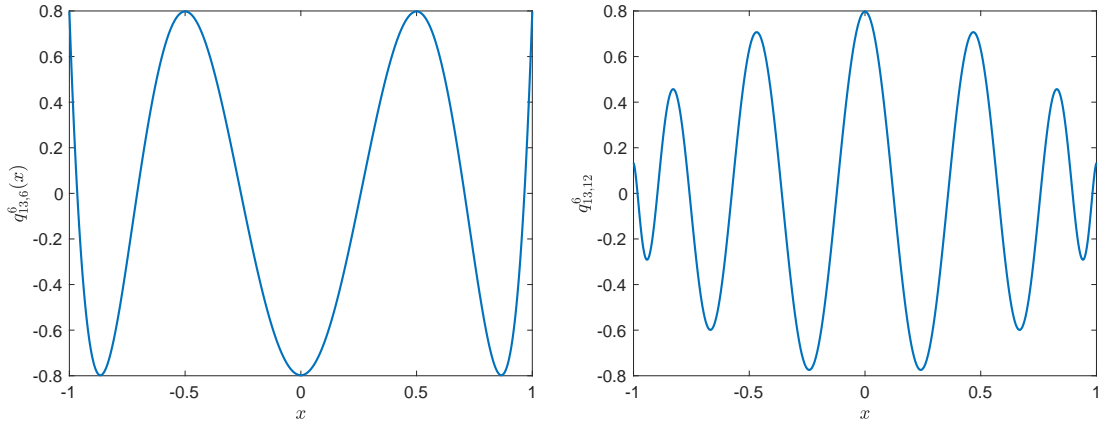


Figure 2: The polynomials  $q_{13,6}^6$  (left) and  $q_{13,12}^6$  (right) .

Note that, like the Chebyshev polynomials, also the orthogonal basis (10) of  $\mathcal{V}_n^m$  is not localized in  $[-1, 1]$ , as shown in Figure 2 where the polynomials  $q_{13,6}^6$  and  $q_{13,12}^6$  are plotted.

**Definition 2.1.** Under the previous notation, we define the orthonormal VP scaling functions as follows

$$\tilde{\varphi}_{n,k}^m(x) := \sum_{r=0}^{n-1} \tau_{r,k}^n q_{n,r}^m(x), \quad k = 1, \dots, n \quad (14)$$

where

$$\tau_{r,k}^n := \sqrt{\frac{\pi}{n \nu_{n,r}^m}} p_r(x_k^n), \quad r = 0, \dots, n-1, \quad k = 1, \dots, n. \quad (15)$$

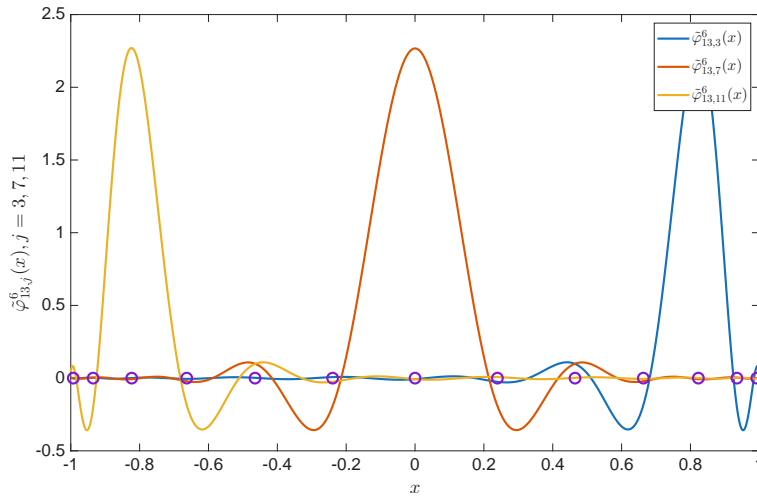


Figure 3: The orthonormal VP scaling functions  $\tilde{\varphi}_{n,k}^m$  for  $n = 13$ ,  $m = 6$ , and  $k = 3, 7, 11$ . The open dots denote the set of nodes  $X_n$ .

Figure 3 displays some plots of the VP scaling polynomials previously defined. We can observe that, contrary to the orthogonal polynomials in (10), the VP scaling

polynomials defined in (14) exhibit a good localization around the Chebyshev nodes. Moreover, they behave very similarly to the interpolatory VP scaling basis defined in [15] (compare Figures 1 and 3) but they are not interpolating anymore. In the following proposition, we state that they constitute an orthonormal basis of  $\mathcal{V}_n^m$ .

**Proposition 2.2.** *We have that  $\mathcal{V}_n^m = \text{span}\{\tilde{\varphi}_{n,k}^m, k = 1, \dots, n\}$  with*

$$\langle \tilde{\varphi}_{n,k}^m, \tilde{\varphi}_{n,h}^m \rangle_{L_w^2} = \delta_{k,h}, \quad k, h = 1, 2, \dots, n. \quad (16)$$

Finally, the next proposition provides the formula for the change of basis from interpolating to orthonormal VP scaling polynomials.

**Proposition 2.3.** *With respect to the interpolating basis (7), the orthonormal scaling functions can be expanded as follows*

$$\tilde{\varphi}_{n,k}^m(x) = \sqrt{\frac{\pi}{n}} \sum_{h=1}^n \left[ \sum_{r=0}^{n-1} \frac{p_r(x_k^n) p_r(x_h^n)}{\sqrt{\nu_{n,r}^m}} \right] \Phi_{n,h}^m(x) \quad k = 1, 2, \dots, n. \quad (17)$$

**Remark 2.4.** *We note that for the opposite change of basis, as an inverse formula of (17), we have*

$$\Phi_{n,h}^m(x) = \left( \sqrt{\frac{\pi}{n}} \right)^3 \sum_{k=1}^n \left[ \sum_{r=0}^{n-1} \sqrt{\nu_{n,r}^m} p_r(x_k^n) p_r(x_h^n) \right] \tilde{\varphi}_{n,k}^m(x), \quad h = 1, 2, \dots, n. \quad (18)$$

*This formula can be easily proved by computing the Fourier coefficients  $\langle \Phi_{n,h}^m, \tilde{\varphi}_{n,k}^m \rangle_{L_w^2}$  by means of (13), (14), and (11).*

### 3. Approximation operators on the sampling space $\mathcal{V}_n^m$

In this section, using the new orthonormal VP scaling basis given in Def. 2.1, we introduce the corresponding Fourier projection on  $\mathcal{V}_n^m$ , denoted by  $S_n^m$ , and a discrete approximation operator on  $\mathcal{V}_n^m$ , denoted by  $\tilde{S}_n^m$ , which we deduce from  $S_n^m$  by approximating the Fourier-like coefficients.

We study their behavior w.r.t. the following norm

$$\|f\|_p := \begin{cases} \sup_{|x| \leq 1} |f(x)| & p = \infty \\ \left( \int_{-1}^1 |f(x)|^p w(x) dx \right)^{\frac{1}{p}} & 1 \leq p < \infty \end{cases} \quad (19)$$

in the functional spaces  $L_w^p = \{f : \|f\|_p < \infty\}$ , with  $1 \leq p \leq \infty$ . In the case  $p = \infty$  we also consider the space  $C^0$  of continuous functions on  $[-1, 1]$  equipped with the sup norm.

Taking into account that  $\mathbb{P}_{n-m} \subseteq \mathcal{V}_n^m \subseteq \mathbb{P}_{n+m-1}$ , we will compare the approximation error with the error of the best polynomial approximation

$$E_n(f)_p := \inf_{P \in \mathbb{P}_n} \|f - P\|_p, \quad 1 \leq p \leq \infty, \quad n \in \mathbb{N}, \quad (20)$$

looking for having a comparable approximation order. With regard to this, we recall that

$$\lim_{n \rightarrow \infty} E_n(f)_p = 0, \quad 1 \leq p \leq \infty \quad (21)$$

holds  $\forall f \in L_w^p$  in the case  $1 \leq p < \infty$  while it holds  $\forall f \in C^0$  if  $p = \infty$ .

Moreover, the convergence order in (21) is strictly connected with the smoothness of the function  $f$  in the space considered, and it is known for several classes of smoothness [2].

That said, as a first operator, let us consider the Fourier projector associated with the new orthonormal VP scaling basis (14) of  $\mathcal{V}_n^m$ . As is well known, such an orthogonal projection is defined by

$$S_n^m f(x) := \sum_{k=1}^n \langle f, \tilde{\varphi}_{n,k}^m \rangle_{L_w^2} \tilde{\varphi}_{n,k}^m(x), \quad |x| \leq 1. \quad (22)$$

Equivalently, in integral form, we have

$$S_n^m f(x) = \int_{-1}^1 s_n^m(x, y) f(y) w(y) dy, \quad s_n^m(x, y) := \sum_{k=1}^n \tilde{\varphi}_{n,k}^m(x) \tilde{\varphi}_{n,k}^m(y). \quad (23)$$

**Remark 3.1.** Note that by Definition 2.1, using the orthogonality of the matrix  $[\sqrt{\frac{\pi}{n}} p_{i-1}(x_j^n)]_{i,j=1,\dots,n}$ , we get

$$\begin{aligned} s_n^m(x, y) &= \frac{\pi}{n} \sum_{k=1}^n \left( \sum_{r=0}^{n-1} \frac{p_r(x_k^n) q_{n,r}^m(x)}{\sqrt{\nu_{n,r}^m}} \right) \left( \sum_{s=0}^{n-1} \frac{p_s(x_k^n) q_{n,s}^m(y)}{\sqrt{\nu_{n,s}^m}} \right) \\ &= \sum_{r=0}^{n-1} \sum_{s=0}^{n-1} \frac{q_{n,r}^m(x) q_{n,s}^m(y)}{\sqrt{\nu_{n,r}^m} \sqrt{\nu_{n,s}^m}} \delta_{r,s}, \end{aligned}$$

i.e., the kernel  $s_n^m(x, y)$  can also be written as follows

$$s_n^m(x, y) = \sum_{r=0}^{n-1} \frac{q_{n,r}^m(x) q_{n,r}^m(y)}{\nu_{n,r}^m}, \quad \forall x, y \in [-1, 1]. \quad (24)$$

Let us first study the asymptotic behavior of the norm of the map  $S_n^m : L_w^p \rightarrow L_w^p$  defined by (22), i.e., let us examine

$$\|S_n^m\|_{L_w^p \rightarrow L_w^p} = \sup_{f \in L_w^p} \frac{\|S_n^m f\|_p}{\|f\|_p}, \quad 1 \leq p \leq \infty.$$

The case  $p = 2$  is trivial since any orthogonal projection in the associated Hilbert space has the norm equal to one, and hence we have

$$\|S_n^m\|_{L_w^2 \rightarrow L_w^2} = 1, \quad \forall n, m \in \mathbb{N} \quad \text{with } m < n. \quad (25)$$

For the other cases, a crucial role is played by the Lebesgue functions  $\lambda_n^m(x)$  and the Lebesgue constants  $\Lambda_n^m$ , defined as

$$\lambda_n^m(x) := \int_{-1}^1 |s_n^m(x, y)| w(y) dy, \quad \Lambda_n^m := \sup_{|x| \leq 1} \lambda_n^m(x). \quad (26)$$

Indeed, by classical arguments of functional analysis, for the limit cases  $p = 1$  and  $p = \infty$ , we have

$$\|S_n^m\|_{L_w^p \rightarrow L_w^p} = \Lambda_n^m, \quad p \in \{1, \infty\}, \quad (27)$$

and using the Riesz–Thorin interpolation theorem (see, e.g., [5, Corollary 2.2]) we also get

$$\|S_n^m\|_{L_w^p \rightarrow L_w^p} \leq \mathcal{C}_p \Lambda_n^m, \quad 1 < p < \infty \quad (28)$$

with  $\mathcal{C}_p > 0$  dependent only on  $p$ .

In Figure 4 we show the Lebesgue functions  $\lambda_n^m(x)$  for  $n = 10, 100$  and  $m = \lfloor \theta n \rfloor$  with  $\theta = 0.5$ .

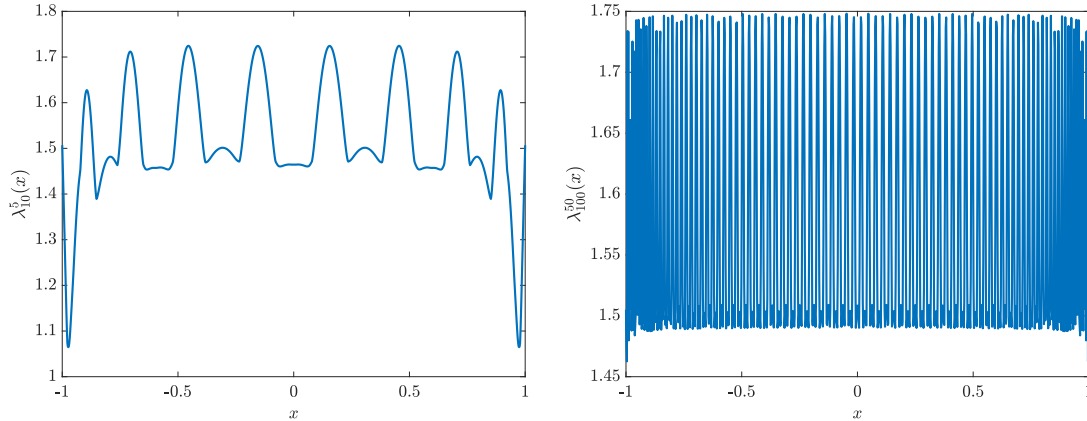


Figure 4: Lebesgue functions  $\lambda_{10}^5(x)$  (left) and  $\lambda_{100}^{50}(x)$  (right).

The following theorem states that, for arbitrarily large  $n \in \mathbb{N}$ , the Lebesgue functions  $\lambda_n^m(x)$  are bounded in  $[-1, 1]$ , uniformly w.r.t.  $n$ .

**Theorem 3.2.** *Let  $\theta \in ]0, 1[$  arbitrarily fixed,  $n \in \mathbb{N}$  arbitrarily large, and  $m = \lfloor \theta n \rfloor$ . The Lebesgue constants defined in (26) satisfy*

$$\sup_n \Lambda_n^m < \infty. \quad (29)$$

As a corollary of the previous result, we have the following

**Corollary 3.3.** *Let  $\theta \in ]0, 1[$  arbitrarily fixed,  $n \in \mathbb{N}$  arbitrarily large, and  $m = \lfloor \theta n \rfloor$ . For any  $1 \leq p \leq \infty$ , the operator map  $S_n^m : L_w^p \rightarrow L_w^p$  defined by (22) is uniformly bounded w.r.t.  $n$ . Moreover, we have*

$$E_{n+m-1}(f)_p \leq \|S_n^m f - f\|_p \leq \mathcal{C} E_{n-m}(f)_p, \quad \forall f \in L_w^p, \quad 1 \leq p \leq \infty \quad (30)$$

where  $\mathcal{C} > 0$  is a constant independent of  $f, n, m$ .

**Remark 3.4.** *Regarding the mapping properties of  $S_n^m : L_w^p \rightarrow L_w^p$ , we point out that, by the previous arguments, for an arbitrary fixed pair of positive integers  $n > m$ , and for  $1 \leq p \leq \infty$ , we have*

$$\|S_n^m f\|_p \leq \mathcal{C} \|f\|_p \quad \text{with} \quad \mathcal{C} = \begin{cases} \Lambda_n^m & p = 1, \infty \\ 1 & p = 2 \\ \mathcal{C}_p \Lambda_n^m & \text{otherwise.} \end{cases} \quad (31)$$

being  $\mathcal{C}_p > 0$  dependent only on  $p$ .

Moreover, taking into account that

$$\|S_n^m f - S_n^m \tilde{f}\|_p \leq \|S_n^m\|_{L_w^p \rightarrow L_w^p} \|f - \tilde{f}\|_p, \quad 1 \leq p \leq \infty$$

the uniform boundedness of the operator  $S_n^m : L_w^p \rightarrow L_w^p$  ensures the well-conditioning. Finally, regarding the consequences of the error estimate (30), we note that, as  $n \rightarrow \infty$ , the choice  $m = \lfloor \theta n \rfloor$  with fixed  $\theta \in ]0, 1[$ , ensures that both  $(n - m)$  and  $(n + m - 1)$  tend to  $\infty$  at the same rate of  $n$ . Consequently, the estimate (30) implies that

$$\|S_n^m f - f\|_p = \mathcal{O}(n^{-a}) \iff E_n(f)_p = \mathcal{O}(n^{-a}), \quad \forall a > 0, \quad 1 \leq p \leq \infty. \quad (32)$$

By the previous results the Fourier projection  $S_n^m f$  provides a near best and well-conditioned approximation of any  $f \in L_w^p$  in the polynomial space  $\mathcal{V}_n^m$ . However, to obtain  $S_n^m f$  we need to compute the integral coefficients in (22), which can be a difficult task. To overcome this problem, we introduce a discrete version of the orthogonal projection  $S_n^m f$ , achieved by applying to the Fourier-like coefficients in (22) the Gauss-Chebyshev quadrature rule on  $n$  nodes

$$\int_{-1}^1 P(x)w(x)dx = \frac{\pi}{n} \sum_{i=1}^n P(x_i^n), \quad \forall P \in \mathbb{P}_{2n-1}. \quad (33)$$

In this way, we define the following discrete version of  $S_n^m f$

$$\tilde{S}_n^m f(x) := \sum_{k=1}^n \left[ \frac{\pi}{n} \sum_{i=1}^n f(x_i^n) \tilde{\varphi}_{n,k}^m(x_i^n) \right] \tilde{\varphi}_{n,k}^m(x), \quad |x| \leq 1. \quad (34)$$

Equivalent forms of this polynomial are the following

$$\tilde{S}_n^m f(x) = \frac{\pi}{n} \sum_{i=1}^n f(x_i^n) s_n^m(x_i^n, x), \quad (35)$$

$$\tilde{S}_n^m f(x) = \sum_{k=1}^n \left[ \left( \frac{\pi}{n} \right)^{\frac{3}{2}} \sum_{h=1}^n f(x_h^n) \sum_{r=0}^{n-1} \frac{p_r(x_k^n) p_r(x_h^n)}{\sqrt{V_{n,r}^m}} \right] \tilde{\varphi}_{n,k}^m(x). \quad (36)$$

For the discrete projection  $\tilde{S}_n^m$  defined by the previous identities, the Lebesgue functions and constants are the following

$$\tilde{\lambda}_n^m(x) := \frac{\pi}{n} \sum_{i=1}^n |s_n^m(x_i^n, x)|, \quad \tilde{\Lambda}_n^m := \sup_{|x| \leq 1} \tilde{\lambda}_n^m(x). \quad (37)$$

Similarly to the case of the Fourier projector, we have

$$\|\tilde{S}_n^m\|_{C^0 \rightarrow C^0} = \tilde{\Lambda}_n^m, \quad \forall n > m \quad (38)$$

and, more specifically, by the definition, for all functions  $f$  we get

$$|\tilde{S}_n^m f(x)| \leq \tilde{\lambda}_n^m(x) \left( \max_{1 \leq i \leq n} |f(x_i^n)| \right), \quad |x| \leq 1. \quad (39)$$

Figure 5 shows the Lebesgue functions  $\tilde{\lambda}_n^m(x)$  for  $n = 10, 100$  and  $m = n/2$ .

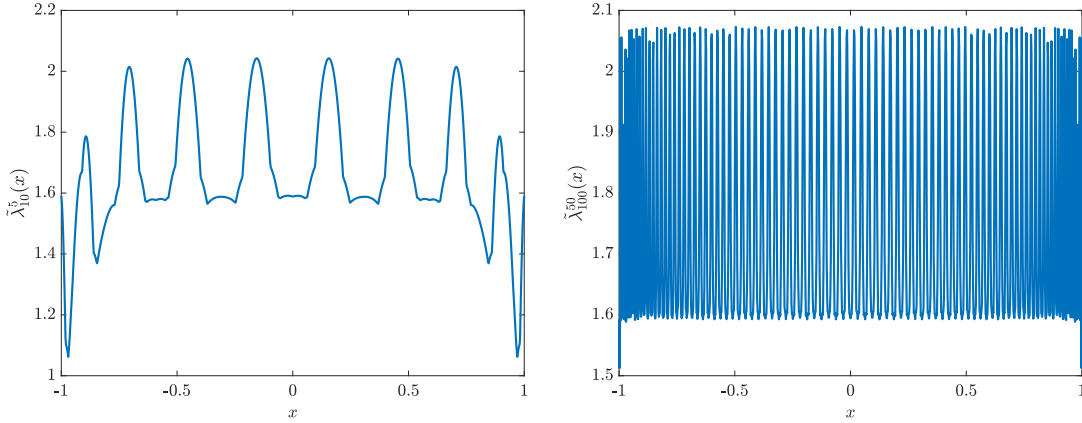


Figure 5: Lebesgue functions  $\tilde{\lambda}_{10}^5(x)$  (left) and  $\tilde{\lambda}_{100}^{50}(x)$  (right) .

Comparing Figure 5 with Figure 4 we note the similar behavior of the Lebesgue functions related to  $\tilde{S}_n^m$  and  $S_n^m$  when  $n = 10, 100$  and  $m = n/2$ . Indeed, such a similar behavior holds more generally for all  $n \in \mathbb{N}$ , as stated below.

**Theorem 3.5.** *For all  $n, m \in \mathbb{N}$  such that  $m = \lfloor \theta n \rfloor$  with fixed  $\theta \in ]0, 1[$ , the Lebesgue functions defined in (26) and (37) satisfy*

$$\mathcal{C}_1 \lambda_n^m(x) \leq \tilde{\lambda}_n^m(x) \leq \mathcal{C}_2 \lambda_n^m(x), \quad |x| \leq 1, \quad (40)$$

where  $\mathcal{C}_1, \mathcal{C}_2 > 0$  are constants independent of  $n, m, x$ .

Note that, taking the supremum w.r.t.  $x \in [-1, 1]$  in (40), we obtain the following inequalities for the associated Lebesgue constants

$$\mathcal{C}_1 \Lambda_n^m \leq \tilde{\Lambda}_n^m \leq \mathcal{C}_2 \Lambda_n^m. \quad (41)$$

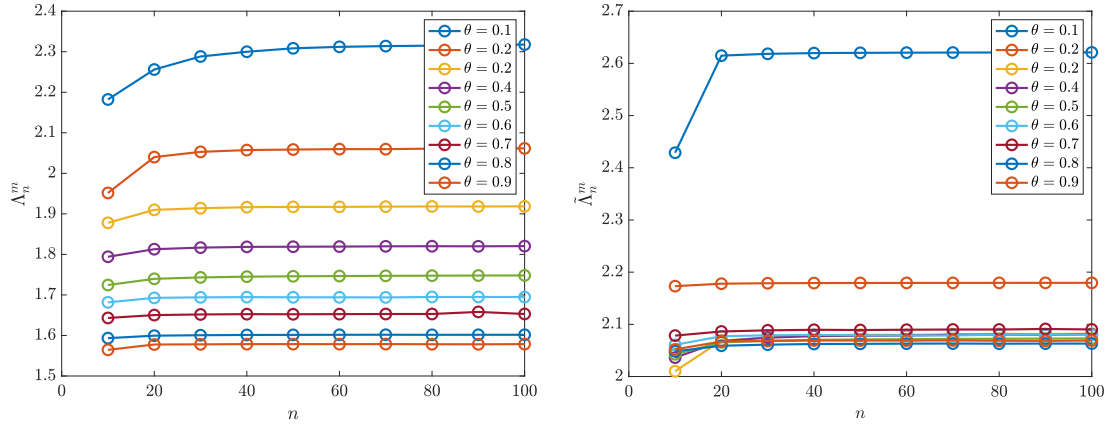


Figure 6: Lebesgue constants  $\Lambda_n^m$  (left) and  $\tilde{\Lambda}_n^m$  (right) for  $n = 10, 20, \dots, 100$  and  $m = \lfloor \theta n \rfloor$  with  $\theta = 0.1, 0.2, \dots, 0.9$ .

Figure 6 shows the Lebesgue constants  $\Lambda_n^m$  and  $\tilde{\Lambda}_n^m$  for  $n = 10, 20, \dots, 100$  and  $m = \lfloor \theta n \rfloor$ , with  $\theta = 0.1, 0.2, \dots, 0.9$ . Relation (41) is confirmed with  $\mathcal{C}_1 = 1$  and we conjecture that  $\Lambda_n^m \leq \tilde{\Lambda}_n^m$  is always true.

Concerning the behavior of the operator  $\tilde{S}_n^m$  in spaces  $L_w^p$  with  $1 \leq p \leq \infty$ , we have to take into account the discrete nature of  $\tilde{S}_n^m$  and, in addition to considering functions defined everywhere, we must replace the continuous norm  $\|f\|_p$  with the following discrete norm

$$\|f\|_{\ell^p(X_n)} := \begin{cases} \max_{1 \leq k \leq n} |f(x_k^n)| & p = \infty \\ \left( \frac{\pi}{n} \sum_{k=1}^n |f(x_k^n)|^p \right)^{\frac{1}{p}} & 1 \leq p < \infty \end{cases} \quad n \in \mathbb{N}$$

in order to get some uniform boundedness result.

We point out that, in general,  $\|f\|_{\ell^p(X_n)}$  is not a norm, but restricted to the polynomials  $f \in \mathcal{V}_n^m$  it is a norm since by (1)-(2),  $\forall f, g \in \mathcal{V}_n^m$ , we have

$$f(x) = g(x), \quad \forall x \in [-1, 1] \iff f(x_i^n) = g(x_i^n), \quad i = 1, \dots, n, \quad (42)$$

which ensures that  $\|f\|_{\ell^p(X_n)} = 0 \implies f = 0, \forall f \in \mathcal{V}_n^m$ .

Using the previous discrete norms, we get the following analog of Corollary 3.3.

**Theorem 3.6.** *Let  $\theta \in ]0, 1[$  arbitrarily fixed,  $n \in \mathbb{N}$  arbitrarily large, and  $m = \lfloor \theta n \rfloor$ . We have*

$$\|\tilde{S}_n^m f\|_p \leq \mathcal{C}_p \|f\|_{\ell^p(X_n)}, \quad 1 \leq p \leq \infty, \quad (43)$$

where  $\mathcal{C}_p > 0$  is a constant that depends only on  $p$ .

Moreover, for all  $f \in C^0$ , the polynomial  $\tilde{S}_n^m f$  uniformly converges to  $f$  as  $n \rightarrow \infty$ , and the near-best error estimate

$$E_{n+m-1}(f)_\infty \leq \|\tilde{S}_n^m f - f\|_\infty \leq \mathcal{C} E_{n-m}(f)_\infty \quad (44)$$

holds with  $\mathcal{C} > 0$  independent of  $f, n, m$ .

**Remark 3.7.** Regarding the value of the constant  $\mathcal{C}_p$  in (43), in proving Theorem 3.6 we state that (78) holds for any pair of integers  $0 < m < n$ .

Finally, recalling the discussion of Remark 3.4, we observe that the error estimate (44) implies the following equivalence

$$\|\tilde{S}_n^m f - f\|_\infty = \mathcal{O}(n^{-a}) \iff E_n(f)_\infty = \mathcal{O}(n^{-a}), \quad \forall a > 0, \quad (45)$$

holds as  $n \rightarrow \infty$  and  $m = \lfloor \theta n \rfloor$  with fixed  $\theta \in ]0, 1[$ .

In conclusion, we have stated that the polynomial  $\tilde{S}_n^m f$ , similarly to the orthogonal projection  $S_n^m f$ , provides a well-conditioned, near-best uniform approximation in the sampling space  $\mathcal{V}_n^m$ , and, contrary to  $S_n^m f$ , it is easily computable once the values of  $f$  are known at the Chebyshev nodes  $X_n$ .

#### 4. Orthonormal VP wavelet functions

Firstly, we recall that in the wavelet space  $\mathcal{W}_n^m$  we have already found the orthogonal basis [15]

$$\tilde{q}_{n,r}^m(x) := \begin{cases} \mu_{n,r}^m p_{2n-r}(x) + \mu_{n,2n-r}^m p_r(x) & n \leq r < n+m \\ p_r(x) & n+m \leq r \leq 3n-m \\ q_{3n,r}^m(x) = \mu_{3n,r}^m p_r(x) - \mu_{3n,6n-r}^m p_{6n-r}(x) & 3n-m < r < 3n \end{cases} \quad (46)$$

satisfying

$$\langle \tilde{q}_{n,r}^m, \tilde{q}_{n,s}^m \rangle_{L_w^2} = v_{n,r}^m \delta_{r,s}, \quad r, s = n, \dots, 3n-1, \quad (47)$$

$$v_{n,r}^m := \begin{cases} \frac{m^2 + (n-r)^2}{2m^2} & n < r < n+m \\ 1 & r = n \text{ or } n+m \leq r \leq 3n-m \\ \frac{m^2 + (3n-r)^2}{2m^2} & 3n-m < r < 3n. \end{cases} \quad (48)$$

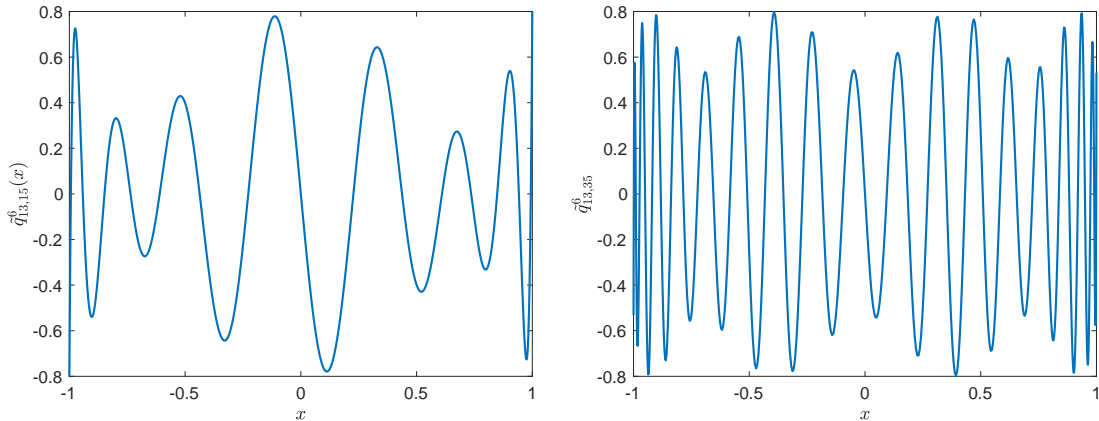


Figure 7: The polynomials  $\tilde{q}_{13,15}^6$  (left) and  $\tilde{q}_{13,35}^6$  (right).

In Figure 7 we show the plots of the polynomials  $\tilde{q}_{13,15}^6$  and  $\tilde{q}_{13,35}^6$ . As we can see, the orthogonal basis polynomials (46) are not localized.

However, in [15] the authors introduce well localized polynomial wavelets  $\psi_{n,k}^m$  that for  $k = 1, \dots, 2n$  constitute a Riesz basis of the detail space  $\mathscr{W}_n^m$ . These wavelets are not orthogonal, but they are interpolating at the nodes

$$Y_{2n} = X_{3n} - X_n = \{y_k^n, k = 1, \dots, 2n\}, \quad n \in \mathbb{N},$$

namely (6) holds. They can be expanded in the orthogonal basis (46) as follows [15]

$$\psi_{n,k}^m(x) = \frac{\pi}{3n} \sum_{r=n}^{3n-1} \rho_{r,k} \tilde{q}_{n,r}^m(x), \quad k = 1, \dots, 2n \quad (49)$$

where

$$\rho_{r,k} := \begin{cases} p_n(y_k^n) & r = n \\ p_r(y_k^n) + p_{|2n-r|}(y_k^n) & n < r \leq 3n - m \quad r \neq 2n \\ p_{2n}(y_k^n) + \sqrt{2}p_0(y_k^n) & r = 2n \\ p_r(y_k^n) + \mu_{n,r-2n}^m p_{r-2n}(y_k^n) - \mu_{n,4n-r}^m p_{4n-r}(y_k^n) & 3n - m < r < 3n. \end{cases} \quad (50)$$

In Figure 8 we show the plots of the VP wavelets  $\psi_{13,4}^6$ ,  $\psi_{13,13}^6$  and  $\psi_{13,23}^6$ , interpolating at the set of nodes  $Y_{26}$  marked with circles.

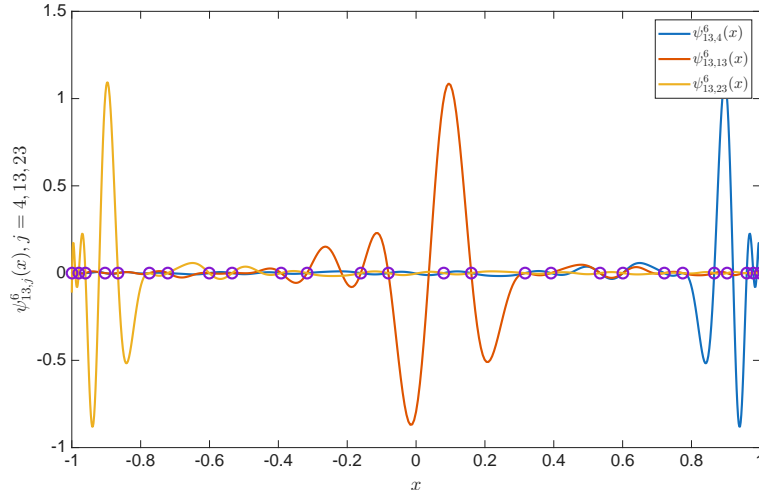


Figure 8: The interpolating VP wavelets  $\psi_{n,k}^m$  for  $n = 13$ ,  $m = 6$ , and  $k = 4, 13, 23$ . The open dots denote the set of nodes  $Y_{2n}$ .

In the following, we define a new wavelet basis of the detail space  $\mathscr{W}_n^m$  that is both well-localized and orthonormal.

**Definition 4.1.** *Under the previous notation, we define the orthonormal VP wavelet functions as follows*

$$\tilde{\psi}_{n,k}^m(x) := \sum_{r=n}^{3n-1} \sigma_{r,k} \frac{\tilde{q}_{n,r}^m(x)}{\sqrt{v_{n,r}^m}}, \quad k = 1, \dots, 2n \quad (51)$$

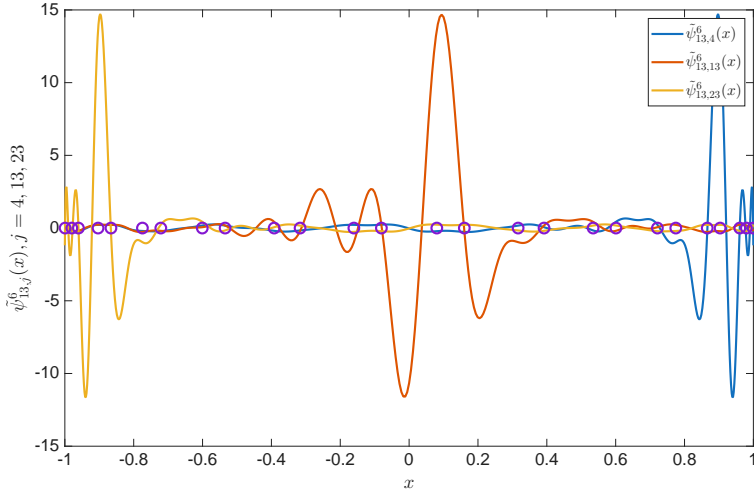


Figure 9: The orthonormal VP wavelets  $\tilde{\psi}_{n,k}^m$  for  $n = 13$ ,  $m = 6$ , and  $k = 4, 13, 23$ . The open dots denote the set of nodes  $Y_{2n}$ .

$$\sigma_{r,k}^n := \sqrt{\frac{\pi}{3n}} \begin{cases} p_n(y_k^n) & \text{if } r = n \\ \frac{p_r(y_k^n) + p_{2n-r}(y_k^n)}{\sqrt{2}} & \text{if } n < r < 2n \\ \frac{p_{2n}(y_k^n) + \sqrt{2} p_0(y_k^n)}{\sqrt{3}} & \text{if } r = 2n \\ \sqrt{\frac{3}{2}} p_r(y_k^n) & \text{if } 2n < r < 3n \end{cases} \quad k = 1, \dots, 2n. \quad (52)$$

In Figure 9 we show the plots of the wavelets  $\tilde{\psi}_{13,4}^6$ ,  $\tilde{\psi}_{13,13}^6$  and  $\tilde{\psi}_{13,23}^6$ . We note similarities with Figure 8 even if the interpolation property on the set of nodes  $Y_{26}$  (marked with empty dots) is no longer valid.

**Proposition 4.2.** *We have that  $\mathscr{W}_n^m = \text{span}\{\tilde{\psi}_{n,k}^m, k = 1, \dots, 2n\}$  with*

$$\langle \tilde{\psi}_{n,k}^m, \tilde{\psi}_{n,h}^m \rangle_{L_w^2} = \delta_{k,h}, \quad k, h = 1, \dots, 2n. \quad (53)$$

## 5. Decomposition and reconstruction

As is well-known, the relation (4) between the approximation and detail spaces establishes a one-to-one correspondence between any function  $f_{3n} \in \mathscr{V}_{3n}^m$  to which a unique pair of functions  $f_n \in \mathscr{V}_n^m$  and  $g_n \in \mathscr{W}_n^m$  corresponds, such that

$$f_{3n}(x) = f_n(x) + g_n(x), \quad \forall x \in [-1, 1]. \quad (54)$$

On the other hand, each function in (54) is uniquely determined by its coefficients in the orthonormal VP scaling or wavelet bases previously defined. To distinguish

such coefficients at any resolution level  $n \in \mathbb{N}$ , we use the following notation

$$f_n(x) = \sum_{k=1}^n a_{n,k} \tilde{\varphi}_{n,k}^m(x), \quad f_n \in \mathcal{V}_n^m \quad (55)$$

$$g_n(x) = \sum_{h=1}^{2n} b_{n,h} \tilde{\psi}_{n,h}^m(x), \quad g_n \in \mathcal{W}_n^m \quad (56)$$

and we set

$$\vec{a}_n := (a_{n,1}, \dots, a_{n,n})^T, \quad \vec{b}_n := (b_{n,1}, \dots, b_{n,2n})^T.$$

The following theorem provides the decomposition/reconstruction formulas to compute  $\vec{a}_n$  and  $\vec{b}_n$  from  $\vec{a}_{3n}$  and vice versa.

**Theorem 5.1.** *For each resolution level  $n \in \mathbb{N}$  and any parameter  $0 < m < n$ , the basis coefficients, defined by (55)–(56), of the functions  $f_{3n} = f_n + g_n$  are related by the matrices  $A = (A_{kj}) \in \mathbb{R}^{n \times 3n}$  and  $B = (B_{hj}) \in \mathbb{R}^{2n \times 3n}$  which are defined by means of the coefficients in (15), (8), (52), and (48), as follows*

$$A_{k,j} := \sum_{s=0}^{n-m} \tau_{s,k}^n \tau_{s,j}^{3n} + \sum_{s=n-m+1}^{n-1} \tau_{s,k}^n [\mu_{n,s}^m \tau_{s,j}^{3n} - \mu_{n,2n-s}^m \tau_{2n-s,j}^{3n}] \quad (57)$$

$$k = 1, \dots, n, \quad j = 1, \dots, 3n$$

$$B_{h,j} := \sum_{r=n}^{n+m-1} \frac{\sigma_{r,h}^n}{\sqrt{v_{n,r}^m}} [\mu_{n,r}^m \tau_{2n-r,j}^{3n} + \mu_{n,2n-r}^m \tau_{r,j}^{3n}] + \sum_{r=n+m}^{3n-m} \frac{\sigma_{r,h}^n}{\sqrt{v_{n,r}^m}} \tau_{r,j}^{3n} \quad (58)$$

$$+ \sum_{r=3n-m+1}^{3n-1} \sigma_{r,h}^n \sqrt{v_{n,r}^m} \tau_{r,j}^{3n} \quad h = 1, \dots, 2n, \quad j = 1, \dots, 3n.$$

These matrices provides the following decomposition and reconstruction formulas

$$\vec{a}_n = A \vec{a}_{3n}, \quad \vec{b}_n = B \vec{a}_{3n} \quad (59)$$

$$\vec{a}_{3n} = A^T \vec{a}_n + B^T \vec{b}_n. \quad (60)$$

Looking at the scalar form of the decomposition/reconstruction formulas (59)–(60) we can note they are primarily based on the following four kinds of transformation:

- **Transform  $\mathcal{T}_n$ :**  $\vec{u} = (u_1, \dots, u_n)^T \in \mathbb{R}^n \rightarrow \mathcal{T}_n \vec{u} = \vec{t} = (t_0, \dots, t_{n-1})^T \in \mathbb{R}^n$  defined by

$$t_r := \sum_{k=1}^n u_k \tau_{r,k}^n, \quad r = 0, \dots, n-1. \quad (61)$$

- **Transform  $\mathcal{T}'_n$ :**  $\vec{t} = (t_0, \dots, t_{n-1})^T \in \mathbb{R}^n \rightarrow \mathcal{T}'_n \vec{t} = \vec{u} = (u_1, \dots, u_n)^T \in \mathbb{R}^n$  defined by

$$u_k := \sum_{r=0}^{N-1} t_r \tau_{r,k}^n, \quad k = 1, \dots, n. \quad (62)$$

- **Transform  $\Sigma_n$ :**  $\vec{u} = (u_1, \dots, u_{2n})^T \in \mathbb{R}^{2n} \rightarrow \Sigma_n \vec{u} = \vec{s} = (s_n, \dots, s_{3n-1})^T \in \mathbb{R}^{2n}$  defined by

$$s_r := \sum_{h=1}^{2n} u_h \sigma_{r,h}^n, \quad r = n, \dots, 3n-1. \quad (63)$$

- **Transform  $\Sigma'_n$ :**  $\vec{s} = (s_n, \dots, s_{3n-1})^T \in \mathbb{R}^{2n} \rightarrow \Sigma'_n \vec{s} = \vec{u} = (u_1, \dots, u_{2n})^T \in \mathbb{R}^{2n}$  defined by

$$u_h := \sum_{r=n}^{3n-1} s_r \sigma_{r,h}^n \quad h = 1, \dots, 2n. \quad (64)$$

Indeed, the scalar version of the formulas (59) and (60) involves double summations, and changing the order of such summations we easily get the next decomposition and reconstruction algorithms based on the previous transformations and on the parameters  $\mu_r := \mu_{n,r}^m$  (cf. (8)) and  $v_r := v_{n,r}^m$  (cf. (48))

---

**Algorithm 1** Decomposition of  $\vec{a}_{3n}$ 


---

**Input:**  $\vec{a}_{3n} = (a_{3n,1}, \dots, a_{3n,3n})^T$   
**Output:**  $\begin{cases} \vec{a}_n = (a_{n,1}, \dots, a_{n,n})^T \\ \vec{b}_n = (b_{n,1}, \dots, b_{n,2n})^T \end{cases}$

- 1: Compute  $\vec{t} = \mathcal{T}_{3n}(\vec{a}_{3n})$
  - 2: **for**  $r = 0 : (n - m)$  **do**
  - 3:    $w_r = t_r$
  - 4: **end for**
  - 5: **for**  $r = (n - m + 1) : (n - 1)$  **do**
  - 6:    $w_r = \mu_r t_r - \mu_{2n-r} t_{2n-r}$
  - 7: **end for**
  - 8:  $\vec{a}_n = \mathcal{T}'_n(\vec{w})$
  - 9: **for**  $r = n : n + m - 1$  **do**
  - 10:    $u_r = \frac{\mu_r t_{2n-r} + \mu_{2n-r} t_r}{\sqrt{v_r}}$
  - 11: **end for**
  - 12: **for**  $r = (n + m) : (3n - m)$  **do**
  - 13:    $u_r = \frac{t_r}{\sqrt{v_r}}$
  - 14: **end for**
  - 15: **for**  $r = (3n - m + 1) : (3n - 1)$  **do**
  - 16:    $u_r = t_r \sqrt{v_r}$
  - 17: **end for**
  - 18:  $\vec{b}_n = \Sigma'_n(\vec{u})$
- 

---

**Algorithm 2** Reconstruction of  $\vec{a}_{3n}$ 


---

**Input:**  $\begin{cases} \vec{a}_n = (a_{n,1}, \dots, a_{n,n})^T \\ \vec{b}_n = (b_{n,1}, \dots, b_{n,2n})^T \end{cases}$   
**Output:**  $\vec{a}_{3n} = (a_{3n,1}, \dots, a_{3n,3n})^T$

- 1: Compute  $\vec{\alpha} = \mathcal{T}_n(\vec{a}_n)$
  - 2: Compute  $\vec{\beta} = \Sigma_n(\vec{b}_n)$
  - 3: **for**  $r = n : 3n - 1$  **do**
  - 4:    $\beta_r = \frac{\beta_r}{\sqrt{v_r}}$
  - 5: **end for**
  - 6: **for**  $r = 0 : (n - m)$  **do**
  - 7:    $t_r = \alpha_r$
  - 8: **end for**
  - 9: **for**  $r = (n - m + 1) : (n - 1)$  **do**
  - 10:    $t_r = \alpha_r \mu_r + \beta_{2n-r} \mu_{2n-r}$
  - 11: **end for**
  - 12:  $t_n = \beta_n$
  - 13: **for**  $r = (n + 1) : (n + m - 1)$  **do**
  - 14:    $t_r = \beta_r \mu_{2n-r} - \alpha_{2n-r} \mu_r$
  - 15: **end for**
  - 16: **for**  $r = (n + m) : (3n - m)$  **do**
  - 17:    $t_r = \beta_r$
  - 18: **end for**
  - 19: **for**  $r = (3n - m + 1) : (3n - 1)$  **do**
  - 20:    $t_r = \beta_r v_r$
  - 21: **end for**
  - 22:  $\vec{a}_{3n} = \mathcal{T}'_{3n}(\vec{t})$
-

Regarding the computational cost of the previous algorithms, we remark that all the transforms in (61)-(64) can be efficiently computed using  $\mathcal{O}(n \log n)$  flops by means of the well-known *discrete cosine transform* (DCT) and its inverse (IDCT), in Matlab known as DCT of type 2 and 3, respectively. We recall that for any pair of vectors  $\vec{v}, \vec{u} \in \mathbb{R}^N$  they are defined as follows

- $\vec{u} = DCT(\vec{v})$  has entries  $u_r = \sqrt{\frac{\pi}{N}} \sum_{k=1}^N v_k p_r(x_k^N)$ ,  $r = 0, \dots, N-1$ ,
- $\vec{u} = IDCT(\vec{v})$  has entries  $u_k = \sqrt{\frac{\pi}{N}} \sum_{r=0}^{N-1} v_r p_r(x_k^N)$ ,  $k = 1, \dots, N$ .

Using these transforms, we have the following algorithms for computing the transforms  $\Sigma_n$  and  $\Sigma'_n$

---

**Algorithm 3** Compute  $\vec{s} = \Sigma_n(\vec{u})$

---

**Input:**  $\vec{u} = (u_1, \dots, u_{2n})^T$

**Output:**  $\vec{s} = (s_n, \dots, s_{3n-1})^T$

```

1: for  $k = 1 : n$  do
2:    $w_{3k-2} = u_{2k-1}$ 
3:    $w_{3k-1} = 0$ 
4:    $w_{3k} = u_{2k}$ 
5: end for
6:  $\vec{x} = DCT(\vec{w})$ 
7:  $s_n = x_n$ 
8: for  $k = n + 1 : 2n - 1$  do
9:    $s_k = \frac{x_k + x_{2n-k}}{\sqrt{2}}$ 
10: end for
11:  $s_{2n} = \frac{x_{2n} + \sqrt{2}x_0}{\sqrt{3}}$ 
12: for  $k = 2n + 1 : 3n - 1$  do
13:    $s_k = \sqrt{\frac{3}{2}}x_k$ 
14: end for

```

---



---

**Algorithm 4** Compute  $\vec{u} = \Sigma'_n(\vec{s})$

---

**Input:**  $\vec{s} = (s_n, \dots, s_{3n-1})^T$

**Output:**  $\vec{u} = (u_1, \dots, u_{2n})^T$

```

1:  $w_0 = \sqrt{\frac{2}{3}}s_{2n}$ 
2: for  $k = 1 : n - 1$  do
3:    $w_k = s_{2n-k}/\sqrt{2}$ 
4: end for
5:  $w_n = s_n$ 
6: for  $k = n + 1 : 2n - 1$  do
7:    $w_k = s_k/\sqrt{2}$ 
8: end for
9:  $w_{2n} = \frac{s_{2n}}{\sqrt{3}}$ 
10: for  $k = 2n + 1 : 3n - 1$  do
11:    $w_k = \sqrt{\frac{3}{2}}s_k$ 
12: end for
13:  $\vec{x} = IDCT(\vec{w})$ 
14: for  $k = 1 : n$  do
15:    $u_{2k-1} = x_{3k-2}$ 
16:    $u_{2k} = x_{3k}$ 
17: end for

```

---

Moreover, using the parameters  $\nu_r := \nu_{n,r}^n$  defined in (12), the transforms  $\mathcal{T}_n$  and  $\mathcal{T}'_n$  can be computed as follows

---

**Algorithm 5** Compute  $\vec{t} = \mathcal{T}_n(\vec{u})$

---

**Input:**  $\vec{u} = (u_1, \dots, u_{2n})^T$

**Output:**  $\vec{t} = (t_0, \dots, t_{n-1})^T$

- 1:  $\vec{t} = DCT(\vec{u})$
  - 2: **for**  $r = n - m + 1 : n - 1$  **do**
  - 3:    $t_r = t_r / \sqrt{\nu_r}$
  - 4: **end for**
- 

---

**Algorithm 6** Compute  $\vec{u} = \mathcal{T}'_n(\vec{t})$

---

**Input:**  $\vec{t} = (t_0, \dots, t_{n-1})^T$

**Output:**  $\vec{u} = (u_1, \dots, u_n)^T$

- 1: **for**  $r = 0 : n - 1$  **do**
  - 2:    $t_r = t_r / \sqrt{\nu_r}$
  - 3: **end for**
  - 4:  $\vec{u} = IDCT(\vec{t})$
- 

In conclusion, we present an example of three decomposition steps for the function

$$f(x) = \sin(6x) + \text{sign}(\sin(x + \exp(2x))),$$

using  $m = \lfloor 0.7n \rfloor$  at each level  $n$ . Starting from  $n = 64 \cdot 3^3 = 1728$ , we first project  $f$  onto  $\mathcal{V}_n^m$  by computing the polynomial approximation  $f_{1728} := \tilde{S}_n^m f$  based on the samples of  $f$  on  $X_n$ . Then we iteratively decompose  $f_{1728}$  as follows

$$\begin{aligned} f_{1728} &= f_{576} + g_{1152} \\ &= f_{192} + g_{384} + g_{1152} \\ &= f_{64} + g_{128} + g_{384} + g_{1152}. \end{aligned}$$

In Figure 10 the function  $f$ , its initial approximation  $f_{1728}$ , the lower degree approximation  $f_{64}$ , and the details  $g_{128}$ ,  $g_{384}$  and  $g_{1152}$  are plotted.

## 6. Comparison with the interpolating case

In Section 3 we have seen that the Fourier projection  $S_n^m f$  associated with the orthonormal VP scaling functions (14), as well as its discrete counterpart  $\tilde{S}_n^m f$ , gives a well-conditioned and near best approximation of  $f$  in the sampling space  $\mathcal{V}_n^m$ .

We recall that similar properties have already been proved in the literature by another projection on  $\mathcal{V}_n^m$  based on the interpolating VP scaling functions (7), and defined by

$$V_n^m f(x) := \sum_{i=1}^n f(x_i^n) \Phi_{n,i}^m(x), \quad \forall x \in [-1, 1]. \quad (65)$$

This polynomial is known in the literature as the VP interpolation polynomial of  $f$  and its approximation properties have been investigated in detail in several papers (see, e.g., [7, 8] and the references therein). Here, we only recall that the results stated in Theorem 3.6 continue to hold by replacing  $\tilde{S}_n^m f$  with the polynomial  $V_n^m f$ , which, in particular, satisfies

$$\|V_n^m f\|_\infty \leq \bar{\Lambda}_n^m \max_{1 \leq k \leq n} |f(x_k^n)|, \quad \bar{\Lambda}_n^m := \max_{|x| \leq 1} \sum_{k=1}^n |\Phi_{n,k}^m(x)|. \quad (66)$$

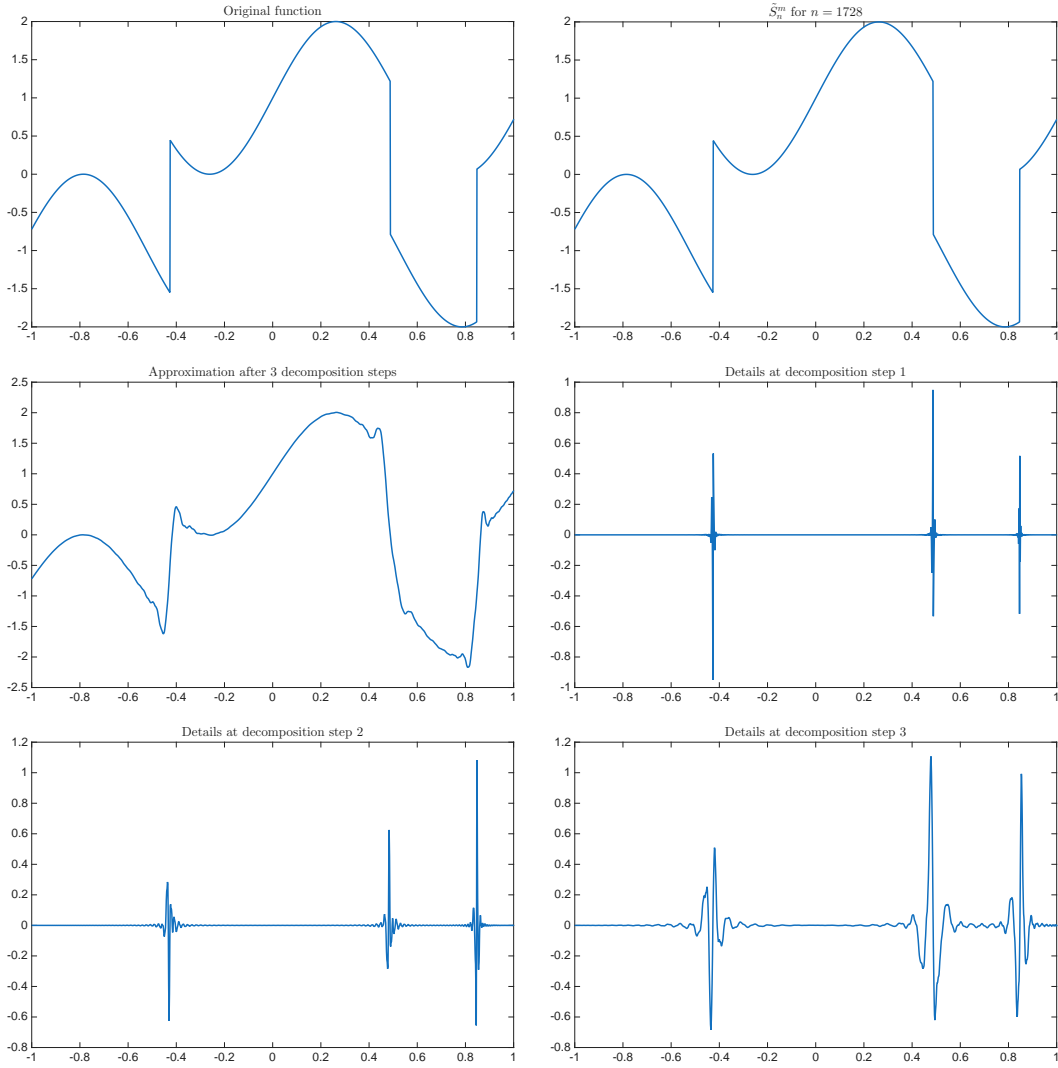


Figure 10: An example of three decomposition steps applied to the approximation  $\tilde{S}_n^m f(x)$  of the function  $f(x) = \sin(6x) + \text{sign}(\sin(x + \exp(2x)))$  with  $n = 1728$  and  $m = \lfloor 0.7n \rfloor$ .

Like the Lebesgue constants  $\Lambda_n^m$  in (26) and  $\tilde{\Lambda}_n^m$  in (37), also the Lebesgue constants  $\bar{\Lambda}_n^m$  in (66) are uniformly bounded w.r.t.  $n$  provided that  $m = \lfloor \theta n \rfloor$  with  $\theta \in ]0, 1[$  arbitrarily fixed (see, e.g., [15, Thm 3.1(e)]). In Figure 11 their behavior is compared for three different values of  $\theta$ .

We note that, by (18), the VP interpolation polynomial (65) can be expanded in the new orthonormal VP scaling basis as follows

$$V_n^m f(x) = \sum_{k=1}^n \left[ \left( \frac{\pi}{n} \right)^{\frac{3}{2}} \sum_{h=1}^n f(x_h^n) \sum_{r=0}^{n-1} \sqrt{\nu_{n,r}^m} p_r(x_k^n) p_r(x_h^n) \right] \tilde{\varphi}_{n,k}^m(x). \quad (67)$$

Comparing (36) and (67) we see the difference between the near best approximation polynomials  $\tilde{S}_n^m f$  and  $V_n^m f$ , both based on the same function values. However, by

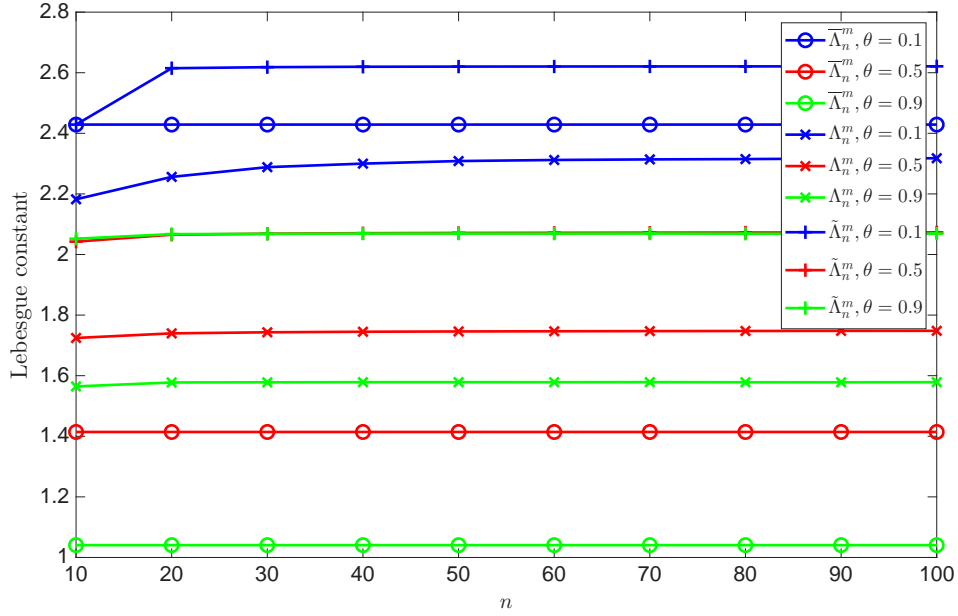


Figure 11: Lebesgue constants  $\bar{\Lambda}_n^m$  (o-),  $\Lambda_n^m$  (-x-), and  $\tilde{\Lambda}_n^m$  (-|-), for  $n = 10, 20, \dots, 100$  and  $m = \lfloor \theta n \rfloor$ , with  $\theta = 0.1$  (blue),  $0.5$  (red),  $0.9$  (green).

(1), the polynomial  $V_n^m f$  also satisfies the interpolation property

$$V_n^m f(x_k^n) = f(x_k^n), \quad k = 1, \dots, n, \quad 0 < m < n. \quad (68)$$

To illustrate the approximation properties of the three approximants,  $V_n^m f(x)$ ,  $S_n^m f(x)$  and  $\tilde{S}_n^m f(x)$ , the approximation error  $E_n^m$  is plotted for the functions  $\sin(x)$  and  $\text{abs}(x)$  in Figure 12, and for the functions  $\text{abs}(x)^{0.3}$  and  $1/(1 + 0.25x^2)$  in Figure 13. The approximation error  $E_n^m$  is defined as

$$E_n^m = \|f_{\text{approx}} - f\|_{\infty},$$

and we take  $m = \lfloor \theta n \rfloor$ , with  $\theta = 0.1, 0.2, \dots, 0.9$  and  $n = 10, 20, \dots, 100$ .

The numerical results show that, for very smooth functions, the errors are very similar, whereas for less regular functions the differences become more pronounced. This is illustrated in the second column of Fig. 12 and in the first column of Fig. 13, where, for higher degrees, the Fourier projection  $S_n^m f$  yields the smallest error, followed by  $\tilde{S}_n^m f$ , whose error is much less sensitive to  $\theta$ , while  $V_n^m f$  gives the largest error.

## 7. Proofs

### 7.1. Proof of Proposition 2.2

Since  $\tilde{\varphi}_{n,k}^m$  are defined as a linear combination of the basis polynomials (10), it is obvious that  $\tilde{\varphi}_{n,k}^m \in \mathcal{V}_n^m$  for all  $k = 1, 2, \dots, n$ . Hence we only have to prove (16).

To this aim we recall that the Darboux kernel

$$K_n(x, y) = \sum_{s=0}^{n-1} p_s(x)p_s(y), \quad x, y \in [-1, 1], \quad n = 0, 1, \dots,$$

satisfies

$$\frac{\pi}{n} K_n(x_k^n, x_h^n) = \delta_{h,k}, \quad h, k = 1, \dots, n.$$

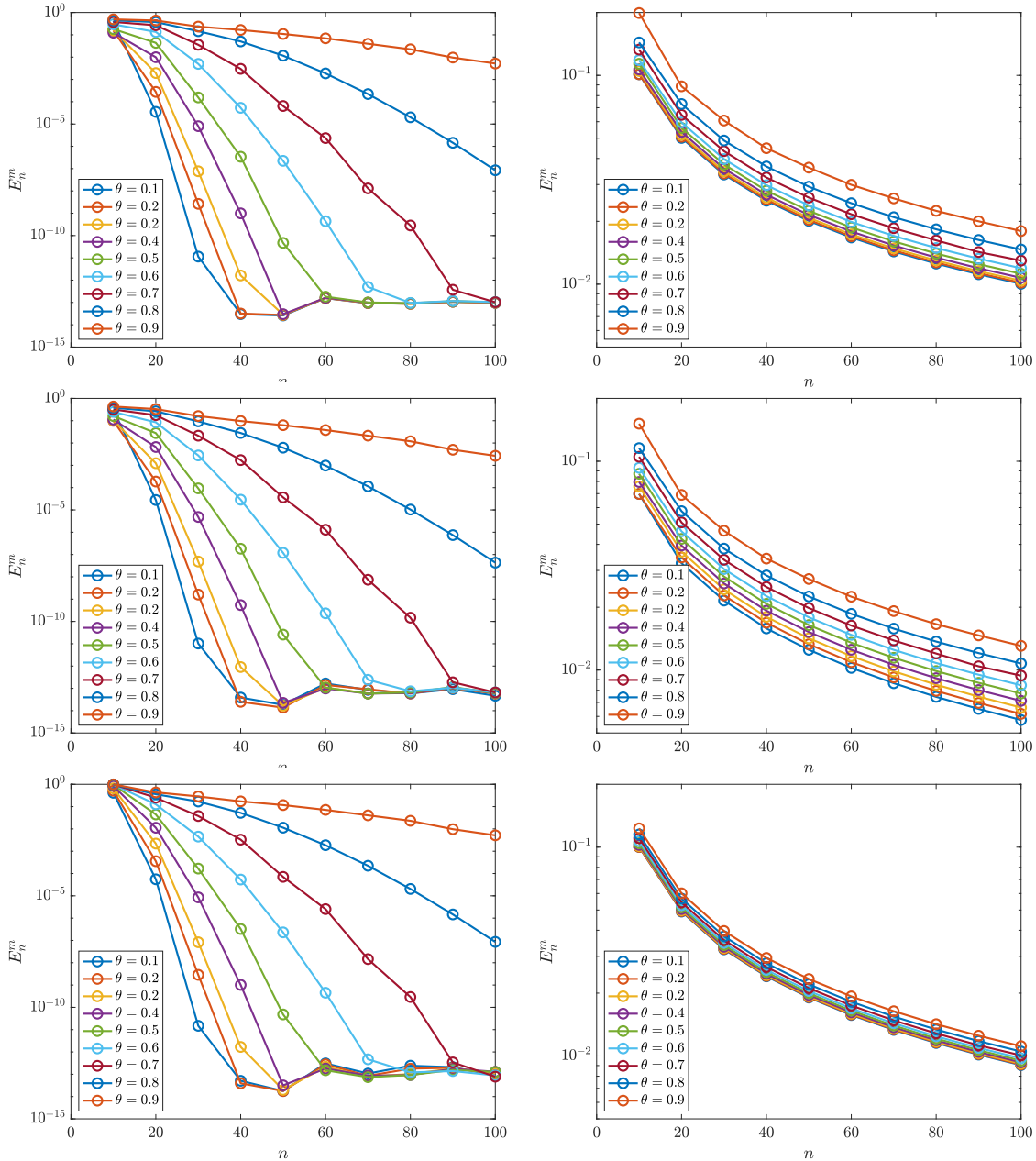


Figure 12: The maximum absolute error  $E_n^m$  for the three approximants  $V_n^m f(x)$  (top),  $S_n^m f(x)$  (middle) and  $\tilde{S}_n^m f(x)$  (bottom) applied to the functions  $f(x) = \sin(x)$  (left) and  $f(x) = \text{abs}(x)$  (right).

Consequently, recalling (14), (15), and (11), we get

$$\begin{aligned} \langle \tilde{\varphi}_{n,k}^m, \tilde{\varphi}_{n,h}^m \rangle_{L_w^2} &= \frac{\pi}{n} \sum_{r=0}^{n-1} \sum_{s=0}^{n-1} \frac{p_r(x_k^n) p_s(x_h^n)}{\sqrt{\nu_{n,r}^m} \sqrt{\nu_{n,s}^m}} \langle q_{n,r}^m, q_{n,s}^m \rangle_{L_w^2} \\ &= \frac{\pi}{n} \sum_{r=0}^{n-1} p_r(x_k^n) p_r(x_h^n) = \delta_{k,h}. \end{aligned}$$

◇

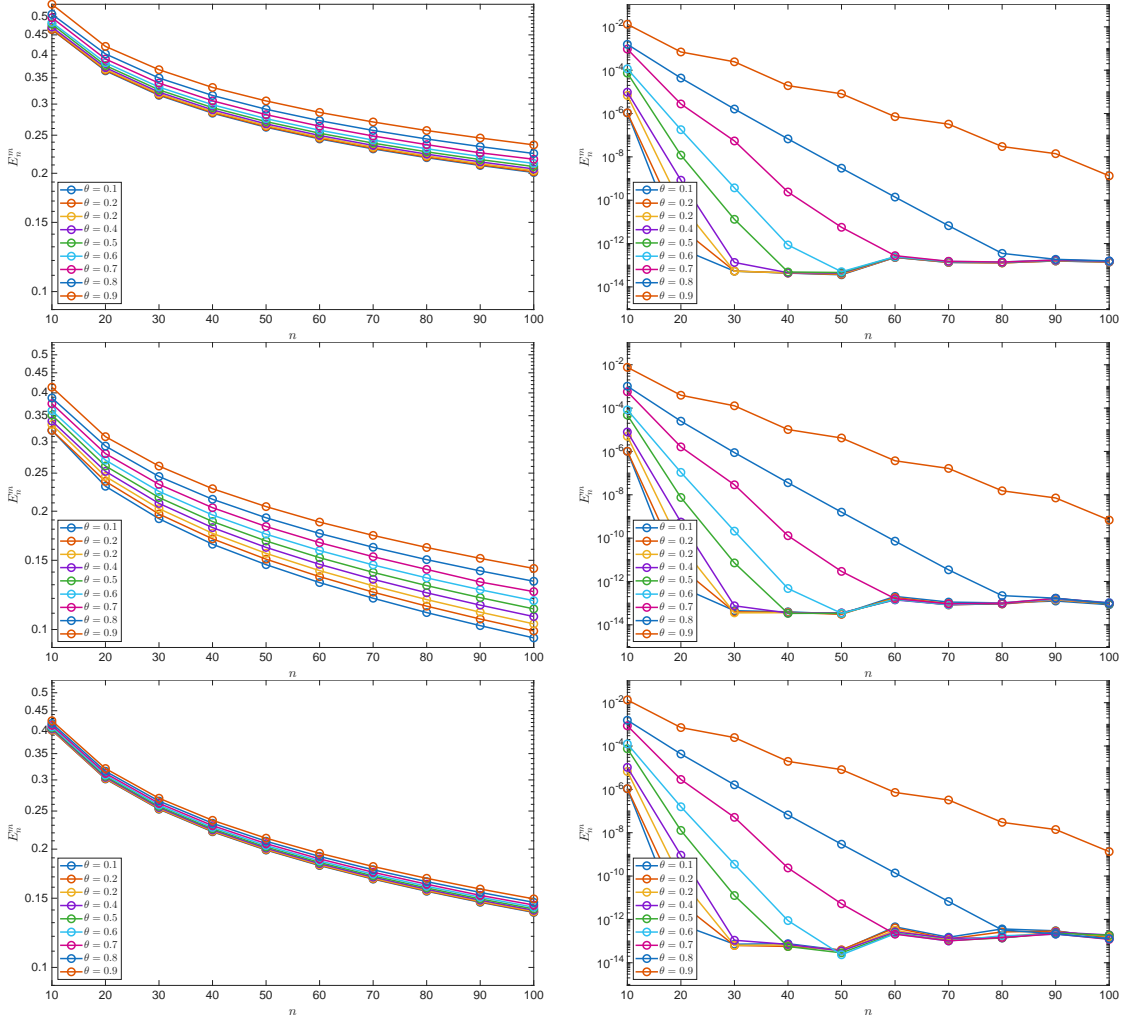


Figure 13: The maximum absolute error  $E_n^m$  for the three approximants  $V_n^m f(x)$  (top),  $S_n^m f(x)$  (middle) and  $\tilde{S}_n^m f(x)$  (bottom) applied to the functions  $f(x) = \text{abs}(x)^{0.3}$  (left) and  $f(x) = 1/(1 + 0.25x^2)$  (right).

### 7.2. Proof of Proposition 2.3

Firstly, note that by the interpolating property of the scaling functions  $\Phi_{n,h}^m$ , we have that

$$f(x) = \sum_{h=1}^n f(x_h^n) \Phi_{n,h}^m(x), \quad \forall f \in \mathcal{V}_n^m.$$

On the other hand, we note that

$$p_{2n-r}(x_h^n) = -p_r(x_h^n), \quad h = 1, \dots, n, \quad r = 1, \dots, n-1, \quad (69)$$

and

$$\mu_{n,r}^m + \mu_{n,2n-r}^m = 1, \quad n-m < r < n,$$

imply that

$$q_{n,r}^m(x_h^n) = p_r(x_h^n), \quad h = 1, \dots, n, \quad r = 0, \dots, n-1. \quad (70)$$

Consequently, we get

$$q_{n,r}^m(x) = \sum_{h=1}^n p_r(x_h^n) \Phi_{n,h}^m(x), \quad r = 0, \dots, n-1. \quad (71)$$

Using this identity and Definition 2.1, we conclude that

$$\tilde{\varphi}_{n,k}^m(x) = \sqrt{\frac{\pi}{n}} \sum_{r=0}^{n-1} \frac{p_r(x_k^n)}{\sqrt{\nu_{n,r}^m}} q_{n,r}^m(x) = \sqrt{\frac{\pi}{n}} \sum_{h=1}^n \left[ \sum_{r=0}^{n-1} \frac{p_r(x_k^n)}{\sqrt{\nu_{n,r}^m}} p_r(x_h^n) \right] \Phi_{n,h}^m(x)$$

holds for  $k = 1, \dots, n$ . ◇

### 7.3. Proof of Theorem 3.2

Firstly, we note that by [15, Thm. 3.1] we have

$$\sup_{|x| \leq 1} \sum_{k=1}^n |\Phi_{n,k}^m(x)| \leq \mathcal{C} \quad (72)$$

with  $\mathcal{C} > 0$  independent of  $n$ .

Consequently, by (26), (24), and (71), we get

$$\begin{aligned} \Lambda_n^m &= \sup_{|x| \leq 1} \int_{-1}^1 |s_n^m(x, y)| w(y) dy = \sup_{|x| \leq 1} \int_{-1}^1 \left| \sum_{r=0}^{n-1} \frac{q_{n,r}^m(x) q_{n,r}^m(y)}{\nu_{n,r}^m} \right| w(y) dy \\ &= \sup_{|x| \leq 1} \int_{-1}^1 \left| \sum_{k=1}^n \Phi_{n,k}^m(x) \sum_{r=0}^{n-1} \frac{p_r(x_k^n) q_{n,r}^m(y)}{\nu_{n,r}^m} \right| w(y) dy \\ &\leq \sup_{|x| \leq 1} \sum_{k=1}^n |\Phi_{n,k}^m(x)| \int_{-1}^1 \left| \sum_{r=0}^{n-1} \frac{p_r(x_k^n) q_{n,r}^m(y)}{\nu_{n,r}^m} \right| w(y) dy \\ &\leq \mathcal{C} \sup_{1 \leq k \leq n} \int_{-1}^1 \left| \sum_{r=0}^{n-1} \frac{p_r(x_k^n) q_{n,r}^m(y)}{\nu_{n,r}^m} \right| w(y) dy. \end{aligned}$$

Hence, to get the statement we have to prove

$$\sup_{1 \leq k \leq n} \int_{-1}^1 \left| \sum_{r=0}^{n-1} \frac{p_r(x_k^n) q_{n,r}^m(y)}{\nu_{n,r}^m} \right| w(y) dy \leq \mathcal{C} \quad (73)$$

where  $\mathcal{C} > 0$  denotes a constant independent of  $n$ .

To this aim, we observe that by (10) and (69), we have

$$\begin{aligned} & \sum_{r=0}^{n-1} \frac{p_r(x_k^n) q_{n,r}^m(y)}{\nu_{n,r}^m} \\ = & \sum_{r=0}^{n-m} p_r(x_k^n) p_r(y) + \sum_{r=n-m+1}^{n-1} \frac{p_r(x_k^n) [\mu_{n,r}^m p_r(y) - \mu_{n,2n-r}^m p_{2n-r}(y)]}{\nu_{n,r}^m} \\ = & \sum_{r=0}^{n-m} p_r(x_k^n) p_r(y) + \sum_{r=n-m+1}^{n-1} \frac{\mu_{n,r}^m}{\nu_{n,r}^m} p_r(x_k^n) p_r(y) + \sum_{r=n-m+1}^{n-1} \frac{\mu_{n,2n-r}^m}{\nu_{n,r}^m} p_{2n-r}(x_k^n) p_{2n-r}(y) \\ = & \sum_{r=0}^{n-m} p_r(x_k^n) p_r(y) + \sum_{r=n-m+1}^{n-1} \frac{\mu_{n,r}^m}{\nu_{n,r}^m} p_r(x_k^n) p_r(y) + \sum_{s=n+1}^{n+m-1} \frac{\mu_{n,s}^m}{\nu_{n,2n-s}^m} p_s(x_k^n) p_s(y), \end{aligned}$$

i.e., recalling (8) and (12), we get

$$\sum_{r=0}^{n-1} \frac{p_r(x_k^n) q_{n,r}^m(y)}{\nu_{n,r}^m} = \sum_{r=0}^{n+m-1} h_r p_r(x_k^n) p_r(y),$$

where we set

$$h_r := \begin{cases} 1 & 0 \leq r \leq n-m \\ m \left( \frac{m+n-r}{m^2 + (n-r)^2} \right) & n-m < r < n+m \\ 0 & \text{otherwise.} \end{cases}$$

Therefore, proving (73) is equivalent to proving

$$\sup_{1 \leq k \leq n} \int_{-1}^1 \left| \sum_{r=0}^{n+m-1} h_r p_r(x_k^n) p_r(y) \right| w(y) dy \leq \mathcal{C}.$$

But this follows from [14, Lemma 5.3] whose assumptions hold since the coefficients  $h_r$  satisfy

$$\sum_{r=0}^{n+m-1} |\Delta^2 h_r| = \mathcal{O} \left( \frac{1}{n} \right)$$

where  $\Delta^2 h_r = \Delta h_{r+1} - \Delta h_r$  and  $\Delta h_r = h_{r+1} - h_r$ . ◇

#### 7.4. Proof of Corollary 3.3

The uniform boundedness result

$$\sup_n \|S_n^m\|_{L_w^p \rightarrow L_w^p} < \infty \quad (74)$$

is a direct consequence of (29), (27) and (28).

The left-hand side inequality in (30) trivially follows from  $S_n^m f \in \mathcal{V}_n^m \subseteq \mathbb{P}_{n+m-1}$  and the definition (20).

To prove the right-hand side in (30), we note that

$$S_n^m P = P, \quad \forall P \in \mathbb{P}_{n-m} \quad (75)$$

follows from  $S_n^m f = f$ ,  $\forall f \in \mathcal{V}_n^m \supseteq \mathbb{P}_{n-m}$ .

Thus, taking  $P^* \in \mathbb{P}_{n-m}$  such that  $\|f - P^*\|_p = E_{n-m}(f)_p$ , we get

$$\|S_n^m f - f\|_p \leq \|S_n^m(f - P^*)\|_p + \|P^* - f\|_p \leq (\|S_n^m\|_{L_w^p \rightarrow L_w^p} + 1)E_{n-m}(f)_p$$

which, due to (74), concludes the proof.  $\diamond$

#### 7.5. Proof of Theorem 3.5.

To prove (40), we recall that in [15, Thm. 3.1 (f)] the following inequalities are proved for the VP interpolation polynomial of any function  $f$  (cf. (65))

$$\mathcal{C}_1 \left( \frac{\pi}{n} \sum_{i=1}^n |f(x_i^n)| \right) \leq \int_{-1}^1 |V_n^m f(y)| w(y) dy \leq \mathcal{C}_2 \left( \frac{\pi}{n} \sum_{i=1}^n |f(x_i^n)| \right) \quad (76)$$

where  $\mathcal{C}_1, \mathcal{C}_2 > 0$  are independent of the specific function  $f$  and also independent of  $n$  and  $m$  in case  $n/m = \mathcal{O}(1)$ , which is certainly verified by our assumption  $m = \lfloor \theta n \rfloor$ .

In the case of functions  $f \in \mathcal{V}_n^m$ , since we have  $V_n^m f = f$ , (76) reduces to

$$\mathcal{C}_1 \left( \frac{\pi}{n} \sum_{i=1}^n |f(x_i^n)| \right) \leq \int_{-1}^1 |f(y)| w(y) dy \leq \mathcal{C}_2 \left( \frac{\pi}{n} \sum_{i=1}^n |f(x_i^n)| \right), \quad \forall f \in \mathcal{V}_n^m.$$

Thus, if we apply (76) to the function  $f_x(y) = s_n^m(y, x)$  with  $x \in [-1, 1]$  arbitrarily fixed, then the statement easily follows by taking into account that  $f_x \in \mathcal{V}_n^m$  is a direct consequence of (24) and  $\mathcal{V}_n^m = \text{span}\{q_{n,r}^m : r = 0, \dots, n-1\}$ .  $\diamond$

#### 7.6. Proof of Theorem 3.6

First of all, we observe that by (33) and (75) we get

$$\tilde{S}_n^m P = S_n^m P = P, \quad \forall P \in \mathbb{P}_{n-m}. \quad (77)$$

So we can proceed as in the proof of Corollary 3.3 to prove (44) using (43) and  $\mathbb{P}_{n-m} \subseteq \mathcal{V}_n^m \subseteq \mathbb{P}_{n+m-1}$ .

Hence, let us prove (43). To this aim, recalling (41), Thm. 3.2 and Cor. (3.3), it is sufficient to prove that we have

$$\|\tilde{S}_n^m f\|_p \leq \mathcal{C} \|f\|_p \quad \text{with} \quad \mathcal{C} = \begin{cases} \tilde{\Lambda}_n^m & p = \infty \\ \Lambda_n^m & p = 1 \\ (1 + 4\pi) \|S_n^m\|_{L_w^{p'} \rightarrow L_w^{p'}} & 1 < p < \infty, \end{cases} \quad (78)$$

with  $\frac{1}{p'} + \frac{1}{p} = 1$ .

In the case  $p \in \{1, \infty\}$ , this easily follows from the definitions that imply the following

$$\begin{aligned} \|\tilde{S}_n^m f\|_\infty &\leq \tilde{\Lambda}_n^m \|f\|_{\ell^\infty(X_n)} \\ \|\tilde{S}_n^m f\|_1 &\leq \left[ \sup_{1 \leq i \leq n} \lambda_n^m(x_i^n) \right] \|f\|_{\ell^1(X_n)} \leq \Lambda_n^m \|f\|_{\ell^1(X_n)}. \end{aligned}$$

In the case  $1 < p < \infty$ , we use dual arguments to get (78). More precisely, recalling that the dual space of  $L_w^p$  is  $L_w^{p'}$ , with  $\frac{1}{p} + \frac{1}{p'} = 1$ , corresponding to any  $\tilde{S}_n^m f$  there exists a function  $g \in L_w^{p'}$  such that  $\|g\|_{p'} = 1$  and we have

$$\begin{aligned} \|\tilde{S}_n^m f\|_p &= \int_{-1}^1 \tilde{S}_n^m f(y) g(y) w(y) dy \\ &= \sum_{i=1}^n f(x_i^n) \int_{-1}^1 s_n^m(x_i^n, y) g(y) w(y) dy \\ &= \frac{\pi}{n} \sum_{i=1}^n f(x_i^n) S_n^m g(x_i^n) \\ &\leq \left( \frac{\pi}{n} \sum_{i=1}^n |f(x_i^n)|^p \right)^{\frac{1}{p}} \left( \frac{\pi}{n} \sum_{i=1}^n |S_n^m g(x_i^n)|^{p'} \right)^{\frac{1}{p'}} \\ &= \|f\|_{\ell^p(X_n)} \left( \frac{\pi}{n} \sum_{i=1}^n |S_n^m g(x_i^n)|^{p'} \right)^{\frac{1}{p'}}. \end{aligned}$$

On the other hand, taking into account that [15, Thm.3.1 (f)]

$$\left( \frac{\pi}{n} \sum_{i=1}^n |F(x_i^n)|^{p'} \right)^{\frac{1}{p'}} \leq (1 + 4\pi) \|F\|_{p'}, \quad \forall F \in \mathcal{V}_n^m,$$

when  $F = \tilde{S}_n^m f$ , we get

$$\begin{aligned} \left( \frac{\pi}{n} \sum_{i=1}^n |S_n^m g(x_i^n)|^{p'} \right)^{\frac{1}{p'}} &\leq (1 + 4\pi) \|S_n^m g\|_{p'} \leq (1 + 4\pi) \|S_n^m\|_{L_w^{p'} \rightarrow L_w^{p'}} \|g\|_{p'} \\ &= (1 + 4\pi) \|S_n^m\|_{L_w^{p'} \rightarrow L_w^{p'}}, \end{aligned}$$

which, by the previous estimate, allows us to conclude that

$$\|\tilde{S}_n^m f\|_p \leq (1 + 4\pi) \|S_n^m\|_{L_w^{p'} \rightarrow L_w^{p'}} \|f\|_{\ell^p(X_n)}, \quad 1 < p < \infty.$$

◇

### 7.7. Proof of Proposition 4.2

Since the polynomials in (46) form an orthogonal basis of  $\mathscr{W}_n^m$ , by Def. 4.1, we certainly have  $\tilde{\psi}_{n,k}^m \in \mathscr{W}_n^m$  for any  $k = 1, \dots, 2n$ . Moreover, by (47) we have

$$\langle \tilde{\psi}_{n,k}^m, \tilde{\psi}_{n,h}^m \rangle_{L_w^2} = \sum_{r=n}^{3n-1} \sigma_{r,k}^m \sigma_{r,h}^m, \quad k, h = 1, \dots, 2n.$$

Hence, to complete the proof and state (53), it is sufficient to prove the orthogonality of the square matrix  $M \in \mathbb{R}^{2n \times 2n}$  defined by

$$M = [M_{r,k}]_{r,k}, \quad M_{r,k} = \sigma_{r,k}^m \quad r = n, \dots, 3n-1, \quad k = 1, \dots, 2n.$$

To this aim, in the following, we prove that

$$\sum_{k=1}^{2n} M_{r,k} M_{s,k} = \delta_{r,s}, \quad r, s = n, \dots, 3n-1. \quad (79)$$

Observe that, by (52), we can write

$$M_{r,k} = \sqrt{\frac{\pi}{3n}} \sigma_r(y_k^n), \quad r = n, \dots, 3n-1, \quad k = 1, \dots, 2n$$

where  $\sigma_r$  denotes the following polynomial of degree at most  $3n-1$

$$\sigma_r(x) = \begin{cases} p_n(x) & \text{if } r = n \\ \frac{p_r(x) + p_{2n-r}(x)}{\sqrt{2}} & \text{if } n < r < 2n \\ \frac{p_{2n}(x) + \sqrt{2} p_0(x)}{\sqrt{3}} & \text{if } r = 2n \\ \sqrt{\frac{3}{2}} p_r(x) & \text{if } 2n < r < 3n \end{cases} \quad x \in [-1, 1].$$

Recalling that  $\langle p_r, p_s \rangle_{L_w^2} = \delta_{r,s}$ , we easily get

$$\langle \sigma_r, \sigma_s \rangle_{L_w^2} = \delta_{r,s} \begin{cases} \frac{3}{2} & 2n < r, s < 3n, \\ 1 & \text{otherwise} \end{cases} \quad r, s = n, \dots, 3n-1. \quad (80)$$

On the other hand, applying the Gaussian rule on the nodes  $X_{3n} = X_n \cup Y_n$ , we obtain

$$\begin{aligned}
\langle \sigma_r, \sigma_s \rangle_{L_w^2} &= \frac{\pi}{3n} \sum_{k=1}^{3n} \sigma_r(x_k^{3n}) \sigma_s(x_k^{3n}) \\
&= \frac{\pi}{3n} \left[ \sum_{k=1}^{2n} \sigma_r(y_k^n) \sigma_s(y_k^n) \right] + \frac{\pi}{3n} \left[ \sum_{k=1}^n \sigma_r(x_k^n) \sigma_s(x_k^n) \right] \\
&= \sum_{k=1}^{2n} M_{r,k} M_{s,k} + \frac{\pi}{3n} \left[ \sum_{k=1}^n \sigma_r(x_k^n) \sigma_s(x_k^n) \right],
\end{aligned}$$

i.e., the following holds

$$\sum_{k=1}^{2n} M_{r,k} M_{s,k} = \langle \sigma_r, \sigma_s \rangle_{L_w^2} - \frac{\pi}{3n} \left[ \sum_{k=1}^n \sigma_r(x_k^n) \sigma_s(x_k^n) \right], \quad r, s = n, \dots, 3n-1. \quad (81)$$

By means of (80) and (81), let us prove (79) by distinguishing the following cases:

- Case  $n \leq s < 3n$  and  $n \leq r \leq 2n$ . Recalling (69) we easily deduce that

$$\sigma_r(x_k^n) = 0 \quad k = 1, \dots, n, \quad n \leq r \leq 2n.$$

Consequently, we get

$$\sum_{k=1}^n \sigma_r(x_k^n) \sigma_s(x_k^n) = 0, \quad n \leq s < 3n, \quad n \leq r \leq 2n,$$

and (80)-(81) imply

$$\sum_{k=1}^{2n} M_{r,k} M_{s,k} = \langle \sigma_r, \sigma_s \rangle_{L_w^2} = \delta_{r,s}, \quad n \leq s < 3n, \quad n \leq r \leq 2n. \quad (82)$$

- Case  $2n < r < 3n$  and  $n \leq s \leq 2n$ . In this case, we have

$$\sigma_s(x_k^n) = 0 \quad k = 1, \dots, n, \quad n \leq s \leq 2n.$$

and analogously to the previous case we get (79).

- Case  $2n < r, s < 3n$ . Let us set

$$r = 3n - \ell_1, \quad s = 3n - \ell_2, \quad \ell_1, \ell_2 = 1, \dots, n-1.$$

Recalling that

$$\cos[(3n - \ell)t] = \cos[(2nt)] \cos[(n - \ell)t] - \sin[(2nt)] \sin[(n - \ell)t]$$

we easily deduce

$$p_{3n-\ell}(x_k^n) = -p_{n-\ell}(x_k^n), \quad \ell = 1, \dots, n-1, \quad k = 1, \dots, n,$$

which implies the following

$$\begin{aligned} \frac{\pi}{n} \sum_{k=1}^n p_r(x_k^n) p_s(x_k^n) &= \frac{\pi}{n} \sum_{k=1}^n p_{3n-\ell_1}(x_k^n) p_{3n-\ell_2}(x_k^n) \\ &= \frac{\pi}{n} \sum_{k=1}^n p_{n-\ell_1}(x_k^n) p_{n-\ell_2}(x_k^n) \\ &= \langle p_{n-\ell_1}, p_{n-\ell_2} \rangle_{L_w^2} = \delta_{\ell_1, \ell_2} = \delta_{r, s}, \end{aligned}$$

having used (33) at the last line.

Consequently, for  $2n < r, s < 3n$  we get

$$\frac{\pi}{3n} \sum_{k=1}^n \sigma_r(x_k^n) \sigma_s(x_k^n) = \frac{\pi}{2n} \sum_{k=1}^n p_r(x_k^n) p_s(x_k^n) = \frac{1}{2} \delta_{r, s},$$

and by (80)-(81) we conclude that

$$\sum_{k=1}^{2n} M_{r, k} M_{s, k} = \langle \sigma_r, \sigma_s \rangle_{L_w^2} - \frac{1}{2} \delta_{r, s} = \delta_{r, s}, \quad 2n < r, s < 3n. \quad (83)$$

◇

### 7.8. Proof of Theorem 5.1

First of all, let us observe that, for all  $x \in [-1, 1]$ , the following two-scale relations

$$\tilde{\varphi}_{n, k}^m(x) = \sum_{j=1}^{3n} \langle \tilde{\varphi}_{n, k}^m, \tilde{\varphi}_{3n, j}^m \rangle_{L_w^2} \tilde{\varphi}_{3n, j}^m(x), \quad k = 1, \dots, n, \quad (84)$$

$$\tilde{\psi}_{n, h}^m(x) = \sum_{j=1}^{3n} \langle \tilde{\psi}_{n, h}^m, \tilde{\varphi}_{3n, j}^m \rangle_{L_w^2} \tilde{\varphi}_{3n, j}^m(x), \quad h = 1, \dots, 2n, \quad (85)$$

trivially follow by expanding  $\tilde{\varphi}_{n, k}^m \in \mathcal{V}_{3n}^m$  and  $\tilde{\psi}_{n, h}^m \in \mathcal{V}_{3n}^m$  in the orthonormal VP scaling basis  $\{\tilde{\varphi}_{3n, j}^m, j = 1, \dots, 3n\}$  of  $\mathcal{V}_{3n}^m$ .

The previous relations are governed by the rectangular matrices

$$\begin{aligned} A &= [A_{k, j}] & A_{k, j} &= \langle \tilde{\varphi}_{n, k}^m, \tilde{\varphi}_{3n, j}^m \rangle_{L_w^2} & k &= 1, \dots, n, & j &= 1, \dots, 3n \\ B &= [B_{h, j}] & B_{h, j} &= \langle \tilde{\psi}_{n, h}^m, \tilde{\varphi}_{3n, j}^m \rangle_{L_w^2} & h &= 1, \dots, 2n, & j &= 1, \dots, 3n. \end{aligned}$$

They form the square matrix  $Q = [Q_{k, j}] \in \mathbb{R}^{3n \times 3n}$  defined as follows

$$Q = \begin{bmatrix} A \\ B \end{bmatrix}, \quad Q_{k, j} = \begin{cases} A_{k, j} & k = 1, \dots, n, \\ B_{k-n, j} & k = n+1, \dots, 3n, \end{cases} \quad j = 1, \dots, 3n.$$

Let us prove that  $Q$  is an orthogonal matrix stating that  $QQ^T = I$ , where  $I$  denotes the identity matrix.

Indeed, taking into account the orthogonality properties stated in (4), Prop. 2.2, Prop. 4.2, and using (84)–(85), we get

$$\begin{aligned}\delta_{h,k} &= \langle \tilde{\varphi}_{n,h}^m, \tilde{\varphi}_{n,k}^m \rangle_{L_w^2} = \sum_{j=1}^{3n} A_{hj}A_{kj} = (AA^T)_{hk}, & h, k = 1, \dots, n \\ \delta_{h,k} &= \langle \tilde{\psi}_{n,h}^m, \tilde{\psi}_{n,k}^m \rangle_{L_w^2} = \sum_{j=1}^{3n} B_{hj}B_{kj} = (BB^T)_{h,k}, & h, k = 1, \dots, 2n, \\ 0 &= \langle \tilde{\psi}_{n,h}^m, \tilde{\varphi}_{n,k}^m \rangle_{L_w^2} = \sum_{j=1}^{3n} B_{hj}A_{kj} = (BA^T)_{hk} = (AB^T)_{kh}, & \begin{array}{l} h = 1, \dots, 2n, \\ k = 1, \dots, n \end{array}\end{aligned}$$

which implies

$$QQ^T = \begin{bmatrix} A \\ B \end{bmatrix} [A^T \ B^T] = \begin{bmatrix} AA^T & AB^T \\ BA^T & BB^T \end{bmatrix} = I. \quad (86)$$

As a consequence of (86), we have that  $Q^{-1} = Q^T$  and the two scale relations (84)–(85) can be inverted simply taking the transpose of the matrices  $A$  and  $B$ . More precisely, in vector notation, setting

$$\vec{\varphi}_n = \begin{bmatrix} \tilde{\varphi}_{n,1}^m(x) \\ \vdots \\ \tilde{\varphi}_{n,n}^m(x) \end{bmatrix} \quad \vec{\psi}_n = \begin{bmatrix} \tilde{\psi}_{n,1}^m(x) \\ \vdots \\ \tilde{\psi}_{n,2n}^m(x) \end{bmatrix}$$

we have the following vector form of the two scale relations

$$\begin{bmatrix} \vec{\varphi}_n \\ \vec{\psi}_n \end{bmatrix} = \begin{bmatrix} A \\ B \end{bmatrix} \vec{\varphi}_{3n} \quad \vec{\varphi}_{3n} = [A^T \ B^T] \begin{bmatrix} \vec{\varphi}_n \\ \vec{\psi}_n \end{bmatrix} \quad (87)$$

that easily implies

$$\begin{bmatrix} \vec{a}_n \\ \vec{b}_n \end{bmatrix} = \begin{bmatrix} A \\ B \end{bmatrix} \vec{a}_{3n} \quad \vec{a}_{3n} = [A^T \ B^T] \begin{bmatrix} \vec{a}_n \\ \vec{b}_n \end{bmatrix}$$

i.e. (59) and (60) hold.

Hence, to complete the proof, it remains to prove that the identities (57) and (58) hold for the entries  $A_{kj}$  and  $B_{hj}$ .

Regarding  $A_{kj}$ , for  $k = 1, \dots, n$  and  $j = 1, \dots, 3n$ , taking into account that

$$\langle q_{n,r}^m, q_{3n,s}^m \rangle_{L_w^2} = \begin{cases} \delta_{r,s} & 0 \leq r \leq n-m, \quad 0 \leq s \leq 3n-m \\ \mu_{n,r}^m \delta_{r,s} - \mu_{n,2n-r}^m \delta_{2n-r,s} & n-m < r < n \quad 0 \leq s \leq 3n-m \\ 0 & 0 \leq r < n \quad 3n-m < s < 3n \end{cases}$$

by (14), we get

$$\begin{aligned}
A_{kj} &= \langle \tilde{\varphi}_{n,k}^m, \tilde{\varphi}_{3n,j}^m \rangle_{L_w^2} = \sum_{r=0}^{n-1} \sum_{s=0}^{3n-1} \tau_{r,k}^n \tau_{s,j}^{3n} \langle q_{n,r}^m, q_{3n,s}^m \rangle_{L_w^2} \\
&= \sum_{r=0}^{n-m} \tau_{r,k}^n \tau_{r,j}^{3n} + \sum_{r=n-m+1}^{n-1} \tau_{r,k}^n [\mu_{n,r}^m \tau_{r,j}^{3n} - \mu_{n,2n-r}^m \tau_{2n-r,j}^{3n}].
\end{aligned}$$

Similarly, with regard to  $B_{hj}$ , with  $h = 1, \dots, 2n$  and  $j = 1, \dots, 3n$ , taking into account that

$$\langle \tilde{q}_{n,r}^m, q_{3n,s}^m \rangle_{L_w^2} = \begin{cases} \mu_{n,r}^m \delta_{2n-r,s} + \mu_{n,2n-r}^m \delta_{r,s} & n \leq r < n+m & 0 \leq s \leq 3n-m \\ \delta_{r,s} & n+m \leq r \leq 3n-m, & 0 \leq s \leq 3n-m \\ 0 & 3n-m < r < 3n & 0 \leq s \leq 3n-m \\ 0 & n \leq r \leq 3n-m & 3n-m < s < 3n \\ v_{n,r}^m \delta_{r,s} & 3n-m < r < 3n & 3n-m < s < 3n \end{cases}$$

from (51) and (14), we deduce

$$\begin{aligned}
B_{h,j} &= \langle \tilde{\psi}_{n,h}^m, \tilde{\varphi}_{3n,j}^m \rangle_{L_w^2} = \sum_{r=n}^{3n-1} \sum_{s=0}^{3n-1} \frac{\sigma_{r,h}^n}{\sqrt{v_{n,r}^m}} \tau_{s,j}^{3n} \langle \tilde{q}_{n,r}^m, q_{3n,s}^m \rangle_{L_w^2} \\
&= \sum_{r=n}^{n+m-1} \frac{\sigma_{r,h}^n}{\sqrt{v_{n,r}^m}} [\mu_{n,r}^m \tau_{2n-r,j}^{3n} + \mu_{n,2n-r}^m \tau_{r,j}^{3n}] + \sum_{r=n+m}^{3n-m} \frac{\sigma_{r,h}^n}{\sqrt{v_{n,r}^m}} \tau_{r,j}^{3n} + \\
&\quad + \sum_{r=3n-m+1}^{3n-1} \frac{\sigma_{r,h}^n}{\sqrt{v_{n,r}^m}} v_{n,r}^m \tau_{r,j}^{3n}.
\end{aligned}$$

◇

## 8. Conclusion

Instead of taking the fundamental VP polynomials as interpolating scaling functions to generate the corresponding VP approximation space, we define orthonormal scaling functions. Similarly, in the associated detail space, we introduce orthonormal wavelets instead of interpolating wavelets. These new bases, like the interpolatory ones, are well localized around the Chebyshev nodes to which they refer; however, they are not generated by dilation and translation of a single mother function.

For this reason, they do not require any special treatment at the boundaries, since they are naturally defined in the interval  $[-1, 1]$ , to which any other compact interval can be mapped. Other peculiar features include the dependence on a free parameter that determines the number of vanishing moments, and a nonstandard multiresolution analysis based on a scaling factor of three rather than two.

In the paper, we derive computationally efficient decomposition and reconstruction algorithms based on the fast discrete cosine transform. Moreover, we study

the approximation properties of the Fourier projection and its discrete counterpart associated with the new orthonormal scaling functions. In particular, for both approximations, we prove the uniform boundedness of the corresponding Lebesgue constants and the uniform convergence to any continuous function with near-best approximation order.

A comparison with VP interpolation reveals better performance of the new approximations in the case of less regular functions. In future work, we will present an application of the new orthonormal VP wavelets to image compression, highlighting the advantages obtained with respect to interpolating VP wavelets and other classical wavelets.

## Funding

The work of the first author was partially supported by GNCS-INDAM. The work of the second author was partially supported by the Fund for Scientific Research–Flanders (Belgium), project G0B0123N.

## References

- [1] M. Cotronei, W. Themistoclakis, and M. Van Barel. A parametric family of polynomial wavelets for signal and image processing. *Journal of Computational and Applied Mathematics*, 482:117317, 2026.
- [2] Z. Ditzian and V. Totik. *Moduli of smoothness*. Springer-Verlag, New York, 1987.
- [3] B. Fischer and J. Prestin. Wavelets based on orthogonal polynomials. *Mathematics of Computation*, 66(220):1593 – 1618, 1997.
- [4] B. Fischer and W. Themistoclakis. Orthogonal polynomial wavelets. *Numerical Algorithms*, 30(1):37 – 58, 2002.
- [5] J. Gustavsson. On interpolation of weighted  $\ell^p$  spaces and Ovchinnikov’s theorem. *Stud. Math.*, 72:237 – 251, 1982.
- [6] D. Occorsio, G. Ramella, and W. Themistoclakis. Image scaling by de la Vallée Poussin filtered interpolation. *Journal of Mathematical Imaging and Vision*, 65(3):513 – 541, 2023.
- [7] D. Occorsio and W. Themistoclakis. On the filtered polynomial interpolation at Chebyshev nodes. *Appl. Numer. Math.*, 166:272–287, 2021.
- [8] D. Occorsio and W. Themistoclakis. Some remarks on filtered polynomial interpolation at Chebyshev nodes. *Dolomites Research Notes on Approximation*, 14(2):68–84, 2021.

- [9] G. Plonka, K. Selig, and M. Tasche. On the construction of wavelets on a bounded interval. *Advances in Computational Mathematics*, 4(1):357 – 388, 1995.
- [10] J. Prestin and K. Selig. Interpolatory and orthonormal trigonometric wavelets. In Y. Zeevi and R. Coifman, editors, *Signal and Image Representation in Combined Spaces*, volume 7 of *Wavelet Analysis and Its Applications*, pages 201–255. Academic Press, 1998.
- [11] W. Themistoclakis. Some interpolating operators of de la Vallée Poussin type. *Acta Mathematica Hungarica*, 84(3):221 – 235, 1999.
- [12] W. Themistoclakis. Uniform approximation on  $[-1, 1]$  via discrete de la Vallée Poussin means. *Numerical Algorithms*, 60(4):593 – 612, 2012.
- [13] W. Themistoclakis. Weighted  $L^1$  approximation on  $[-1, 1]$  via discrete de la Vallée Poussin means. *Mathematics and Computers in Simulation*, 147:279 – 292, 2018.
- [14] W. Themistoclakis and M. Van Barel. Generalized de la Vallée Poussin approximations on  $[-1, 1]$ . *Numerical Algorithms*, 75(1):1 – 31, 2017.
- [15] W. Themistoclakis and M. Van Barel. A free parameter dependent family of polynomial wavelets on a compact interval. *Numerical Algorithms*, 2025.